UNIVERSITÀ DEGLI STUDI DI MESSINA
DIPARTIMENTO DI SCIENZE CHIMICHE, BIOLOGICHE, FARMACEUTICHE ED AMBIENTALI

DOTTORATO DI RICERCA IN
BIOLOGIA APPLICATA E MEDICINA SPERIMENTALE
XXIX CICLO

Anti-oxidant and anti-inflammatory activities of a flavonoid-rich extract from *Citrus bergamia* Risso et Poiteau juice in both *cell-free* and *in vitro* models

TESI DI DOTTORATO:
DOTT.SSA SANTA CIRMI

TUTOR:
PROF. MICHELE NAVARRA

COORDINATORE DEL CORSO DI DOTTORATO
CHIAR.MO PROF. SALVATORE CUZZOCREA

TRIENNIO 2014-2016

ABSTRACT

Inflammation consists in a series of biological reactions induced by the alteration of tissue homeostasis occurring in response to biological, chemical or physical agents in the organism. Oxidative stress is defined as an imbalance between production and elimination of free radicals and reactive metabolites (oxidants). This is a natural physiological process where the presence of ROS overpowers the cellular radical scavenging ability, thus creating an imbalance in the oxidative status between the oxidants and the anti-oxidants.

Inflammation and oxidative stress are closely related pathophysiological events that are strongly linked each other. One of them may appear before or after the other, but when one emerges the other one is most likely to follow, and then both of them take part in the pathogenesis of many disorders.

In recent years, there has been an extraordinary increase in the number of studies on anti-oxidant properties of various phytochemicals, able to counteract reactive species (RS) overproduction. Among these, flavonoids have been extensively studied mainly for their anti-oxidant property which ameliorates many inflammatory diseases and was linked to the maintenance of good health. *Citrus* fruits and their juices are the main food sources of flavonoids which exert protective effects against numerous degenerative processes. In the last decade a number of studies have investigated the anti-oxidant and anti-inflammatory effects of each single *Citrus* flavonoid as pure compounds. However, few studies have focused on the pharmacological activity of *Citrus* juices and extracts and its molecular mechanisms underlying their potential beneficial effects.

On these bases during my PhD, I focused on the anti-oxidant activity of a flavonoid-rich extract from *Citrus* bergamia juices (BJe) and its effect against inflammatory processes. First, we tested the anti-oxidant properties of BJe in *cell-free* experimental models by ORAC, DPPH, Folin-Ciocalteu and Reducing Power assays, proving its anti-oxidant activity. Then, we assayed its ability to prevent the cytotoxic effects induced by H_2O_2 or $Fe_2(SO_4)_3$. Our results provided evidences that BJe reduces cell death, generation of ROS and membrane lipid peroxidation, improve mitochondrial functionality and prevents DNA-oxidative damage in A549 cells incubated with H_2O_2. Moreover, BJe is able to both induce catalase expression and increase its activity. Furthermore, evidences, that BJe prevents the cytotoxic effects by $Fe_2(SO_4)_3$, have suggested that this extract could possess chelating properties. This hypothesis was confirmed by measuring the presence of redox-active iron in the cells pre-treated with the extract and then exposed to the metal.

In the light of these observations, we wondered whether BJe may be effective against inflammatory processes. To this aim, we used THP-1 monocytes to investigate the mechanisms underlying the beneficial potential of BJe against two different models of inflammation in which the THP-1 cells were exposed to LPS or amyloid-beta$_{1–42}$ (A$\beta_{1–42}$). Exposure of THP-1 cells to BJe inhibited both gene expression and secretion of LPS-induced pro-inflammatory cytokines (IL-6, IL-1β, TNF-α) by a mechanism involving the inhibition of NF-κB activation. In addition, BJe treatment reversed the LPS-enhanced acetylation of p65 in THP-1 cells. Furthermore, increasing concentrations of Sirtinol were able to suppress the inhibitory effect of BJe via p65 acetylation, underscoring that NF-κB-mediated inflammatory cytokine production may be directly linked to SIRT1 activity.

Treatment of THP-1 cells with $A\beta_{1-42}$ significantly induced the expression and secretion of IL-6 and IL-1β in THP-1 cells and increased the phosphorylation of ERK 1/2 as well as p46 and p54 members of JNK family. Moreover, $A\beta_{1-42}$ raised AP-1 DNA binding activity in THP-1-treated cells. Interestingly, all these effects were reduced in the presence of BJe.

In conclusion, our studies provided evidences that BJe may be used in preventing oxidative cell injury suggesting a promising role as a natural drug against inflammatory processes. In addition, the complex mixture of phytochemicals present in the whole extract acts better than the single constituent. This is because all molecules present in a phytocomplex can modulate simultaneously different targets of action in both human cells and microorganisms, leading to a pool of pharmacological effects contributing together to improve patient's health.

Key words: oxidative stress, inflammation, bergamot juice extract, flavonoids, hydrogen peroxide, iron, lipopolysaccharide (LPS), amyloid-beta.

INDEX

1.INTRODUCTION

1.1. The inflammation

Inflammation consists in a series of biological reactions induced by the alteration of tissue homeostasis occurring in response to biological, chemical, or physical agents in the organism (Medzhitov et al., 2008). The classical key features of inflammation are redness, warmth, swelling and pain. Inflammation can be either acute or chronic, depending on the type of stimulus and the effectiveness of the inflammatory process resolution. Acute inflammation begins quickly and persists few hours or few days. It is characterized by the exudation of fluid and plasma proteins as well as leukocyte migration (mainly neutrophils). When the immune system successfully eliminates damaging agents in acute inflammation, the reaction disappears. However, if the inflammatory response fails to remove its cause, a chronic phase occurs. Inflammation cascades can lead to the development of chronic diseases such as asthma, rheumatoid arthritis, multiple sclerosis, inflammatory bowel disease and psoriasis. Chronic inflammation is associated with the presence of lymphocytes and macrophages, vascular proliferation, fibrosis, and tissue destruction. Experimental and clinical studies together with epidemiological observations have identified both chronic infections and inflammation as major risk factors for various types of cancer. It has been estimated that the underlying infections and inflammatory reactions are linked to 15-20% of all cancer deaths (Mantovani et al., 2008). The inflammatory response is characterized by coordinated activation of various signaling pathways that regulate expression of both pro- and anti-inflammatory mediators in cells of inflamed tissue as well as leukocytes recruited from the blood. The nuclear transcription factor κB (NF-κB) is the master

regulator of the inflammatory response, that drives the activation of genes associated with the transcription of inflammatory mediators, such as interleukins, tumor necrosis factor (TNF) and prostaglandins (PGs), as well as inflammatory enzymes, like inducible nitric oxide synthase (iNOS) and cyclooxygenases (COXs).

1.2. The radical species

Radical species (RS), including reactive oxygen species (ROS) and reactive nitrogen species (RNS), are highly reactive molecules physiologically produced in a tightly-regulated manner and in small quantity during the cellular metabolism in aerobic organisms. They are involved in cell homeostasis and control several cellular functions such as signal transduction and gene expression (Kumar and Pandey, 2015). In physiological condition, ROS and RNS are removed quickly by the endogenous anti-oxidant systems such as glutathione peroxidase (GSH-Px), superoxide dismutase (SOD) and catalase (CAT), as well as exogenous anti-oxidant introduced by diet, like vitamin C and E, carotenoids and polyphenols. Imbalance between generation and elimination of RS, due to their overproduction or reduced metabolization can lead to the damage of important cellular and molecular structures such as DNA, proteins, and lipids (Duračková et al., 2010). This can cause pathological conditions (apoptosis, necrosis, uncontrolled cell proteolysis, oxidative DNA damage, lipid peroxidation, etc.) which govern a wide array of diverse disorders (Beckman and Ames, 1998; Golden et al., 2002). Under pathological inflammatory status, there may be exaggerated generation of RS that can diffuse out of the cells, inducing localized oxidative stress and tissue injury (Fialkow et al., 2007). Moreover, the activated phagocytic cells produce large amounts of ROS and RNS. Once generated, they can further generate other RS, leading

to extensive damage. At the onset of inflammation, the infection or tissue damage is sensed by pattern recognition receptors like toll-like receptors (TLR), NOD-like receptors (NLR), and the receptor for advanced glycation end products (RAGE). The stimulation of these receptors upon binding with specific molecules leads to the activation of transcription factors such as nuclear factor-κB (NF-κB) and activating protein-1 (AP-1), that in turn induce pro-inflammatory gene expression, exert antimicrobial functions and recruit additional immune cells (Tabas et al., 2015; Bierhaus et al., 2005). It has been demonstrated that RS (i.e., hydrogen peroxide) can induce inflammation through activation of these same transcription factors (Oliveira-Marques et al., 2009; Vollgraf et al., 1999; Kang et al., 2011).

1.3. Oxidative stress and inflammation

Oxidative stress is defined as an imbalance between production and elimination of free radicals and reactive metabolites (oxidants). This is a natural physiological process where the presence of ROS overpowers the cellular radical scavenging ability, thus creating an imbalance between the oxidants and the antioxidants.

Inflammation and oxidative stress are closely related pathophysiological events that are strongly linked with each other. One of them may appear before or after the other, but when one emerges the other one is most likely to follow, and then both take part in the pathogenesis of many disorders. Nowadays, it is clear that the prolonged low-grade inflammatory process plays a central role in the pathogenesis of many chronic diseases (Cotran et al., 1999). On the other hand, epidemiological and experimental studies strongly suggest a contribution of oxidative stress in many human diseases (Cotran et al., 1999). Just as the inflammatory process can induce oxidative stress, the

latter can cause inflammation through activation of multiple pathways (Castellani et al., 2014; Mittal et al., 2014). The result is that both inflammation and oxidative stress are associated with a number of chronic diseases, including diabetes, hypertension, cardiovascular diseases, neurodegenerative diseases, alcoholic liver disease, chronic kidney disease, cancer and aging (Biswas et al., 2007; Ambade et al., 2012; Biswas et al., 2008; Cachofeiro et al., 2008).

1.4. Natural products for the treatment of inflammation

Several classes of medicines, including corticosteroids, nonsteroidal anti-inflammatory drugs (NSAIDs) and biologic drugs are used to treat the inflammatory disorders. However, they possess several side effects and the biologics ones are expensive to be used. To limit these drawbacks of both synthetic and biologic drugs, over the past three decades, the use of herbal medicines, nutraceuticals and food supplements has greatly increased as an alternative and/or complementary medicine to treat several pathologies, including inflammation (Marino et al., 2015). Indeed, although natural products are not devoid of risk, generally they are safer than both synthetic and biologic drugs. Nowadays, about 80% of people around the world use natural products for the prevention and treatment of many diseases, mainly for their relative safety, efficacy and low cost as well as the compliance by patients. Plants have been the basis of many traditional medicines throughout the world for thousands of years, and continue to provide mankind with new remedies (Dias set al., 2012). In this field, natural products offer great hope in the identification of bioactive molecules useful for the treatment of inflammatory diseases, as it happened for aspirin, the first discovered NSAID, which is still one of the bestselling drug in the world.

In recent years there has been an extraordinary increase in the number of studies on anti-oxidant properties of various phytochemicals, able to counteract RS overproduction. Among these, flavonoids, a family of polyphenols found especially in fruits, vegetables, red wine and tea, have been extensively studied manly for their anti-oxidant property (Rice-Evans et al., 1997; Ross and Kasum, 2002). Flavonoids are plant secondary metabolites commonly found in the fruits and vegetables regularly consumed by humans. Their anti-oxidant activity ameliorates many inflammatory diseases and was linked to the maintenance of good health (Di Matteo and Esposito, 2003; Yao et al., 2004). Several mechanisms are involved in the beneficial effects exerted by flavonoids, including the free radicals scavenging (Kumar and Pandey, 2013), the transition metal ions chelation (Mladěnka et al., 2011), the enhancement of glutathione content, and modulation of defense genes expression via the Nrf2/ARE pathway (Kumar and Pandey, 2013; Chen and Kong, 2005; Masella et al., 2005; Kumar et al., 2014).

1.5. The *Citrus bergamia* Risso et Poiteau

Citrus fruits and their juices are the main food sources of flavonoids and have been extensively studied as regards their cardiovascular, anticancer, anti-infective, neuroprotective, and anti-inflammatory activity (Benavente-Garcıa and Castillo, 2008; Cirmi et al., 2016a; Cirmi et al., 2016b; Cirmi et al., 2016c; Ferlazzo et al., 2016a).

In recent years has gained ground scientific interest in *Citrus bergamia* (bergamot) derivatives. *Citrus bergamia* Risso et Poiteau, also known as “Bergamot,” is a plant belonging to the Rutaceae family. *Citrus bergamia* is defined as a hybrid between a sour orange (*C. aurantium* L.) and lemon (*C. limon* L. Burm. f.) or a mutation of the

latter. Other Authors considered it as a hybrid between a sour orange and lime (*C. aurantifolia* [Christm. and Panzer] Swingle). The botanical and ethno-pharmacological issues of this plant have been reported by Rapisarda and Germanò (2013).

Bergamot fruit is used especially for the extraction of its essential oil (BEO) from the peel (by cold pressing), while the bergamot juice (BJ), derived from squeezing the endocarp of the fruits is considered a byproduct of the BEO's production. Finally, the scraps of bergamot fruit after both BEO extraction and BJ juicing is named "bergamot pastazzo" and it is used as animal feed. BEO is typically used in the cosmetic industry, being found in the composition of many fragrances, body lotions, soaps and so on. It is also used by the food industries (for flavoring tea, beverages and typical Calabrian pastries), by the pharmaceutical industries (to absorb the unpleasant smell of medicinal products and for its antiseptic and antibacterial properties (Cirmi et al., 2016a) and in aromatherapy (Navarra et al., 2015). Recently, BEO has been experimentally investigated for its potential anti-proliferative (Celia et al., 2013; Navarra et al., 2015) and neuroprotective effects (Corasaniti et al., 2007).

Over the last decade, some researchers have started to investigate the biological properties of bergamot derivatives, obtaining important scientific achievements. Studies performed by Miceli et al. (2007) have shown that a chronic administration of BJ is effective to prevent the diet-induced hyperlipidemia in rat, suggesting a relationship between the beneficial effect and its anti-oxidant properties. Moreover, a clinical research showed that the bergamot-derived polyphenolic fraction, given orally in patients suffering from metabolic syndrome, reduced plasma lipids and improved the lipoprotein profile (Mollace et al., 2011; Toth et al., 2016), strengthen the finding obtained in animal model.

Finally, the research group coordinated by prof. Michele Navarra demonstrated that BJ reduces the growth rate of different cancer cell lines by different molecular mechanisms, depending on cancer type. In SH-SY5Y human neuroblastoma cells, BJ stimulated the cell cycle arrest in the G1 phase without inducing apoptosis, and caused a modification in cellular morphology associated with a marked increase in detached cells. The inhibition of adhesive ability onto different physiologic substrates and onto endothelial cell monolayer was correlated to BJ-induced impairment of actin filaments and with the reduction in the expression of the active form of FAK, in turn causing inhibition of cell migration (Delle Monache et al., 2013). Contrariwise, in human hepatocellular carcinoma HepG2 cells, BJ reduced the growth rate through the involvement of p53, p21, and NF-κB pathways, as well as the activation of both intrinsic and extrinsic apoptotic pathways (Ferlazzo et al., 2016b). Moreover, BJ-induced reduction of both cell adhesiveness and motility could be responsible for the slight inhibitory effects on lung metastasis colonization observed in an animal model of spontaneous neuroblastoma metastasis formation in SCID mouse (Navarra et al., 2014). In order to assess which bioactive component of BJ was responsible for its antitumor activity, Visalli et al., (2014) focused on the flavonoid-rich fraction from bergamot juice (BJe). Results suggested that BJe inhibits HT-29 human colorectal carcinoma cell growth and induces apoptosis through multiple mechanisms. Molecular assays revealed that higher concentrations of BJe increase ROS production, which causes a loss of mitochondrial membrane potential and oxidative DNA damage. Lower concentrations of BJe inhibited MAPK pathways and modified apoptosis-related proteins, which in turn induced cell cycle arrest and apoptosis (Visalli et al., 2014).

2. AIM OF RESERCH

Natural products have been shown to exert beneficial effects on human health, as well as it is known that flavonoids can exert protective effects against numerous degenerative processes. In addition, a number of studies have investigated the anti-oxidant and anti-inflammatory effects of single *Citrus* flavonoids as pure compounds. However, few studies have focused on the pharmacological activity of *Citrus* juices and extracts. Moreover, in recent years, *Citrus bergamia* fruit has attracted attention of the scientific community because of its potential to prevent or counteract some pathologies. On the basis of what has been discussed in the introduction section, during my PhD, I evaluated the anti-oxidant and anti-inflammatory effect of BJe in different *cell-free* and *cell-based* experimental models.

3. MATERIALS AND METHODS

3.1. Flavonoid-rich extract from bergamot juice

The flavonoid-rich extract of bergamot juice (BJe) was provided by the company "Agrumaria Corleone" (Palermo, Italy). The fruits of *Citrus bergamia* Risso & Poiteau came from crops located in the province of Reggio Calabria (Italy). The extract was transformed into a dry powder using the spray drying method. Small aliquots of BJe were stored at -20°C. Finally, the drug was defrosted, diluted in culture media, the pH was adjusted to 7.4 and filtered just prior to use.

3.2. Chemical characterization of BJe

BJe powder was dissolved in methanol to a concentration of 1 mg/ml^{-1}, ultra-sonicated and filtered through a 0.2 μm nylon membrane (Millipore, Milan, Italy), and then injected into a UHPLC coupled online to an LCMSIT-TOF mass spectrometer (Shimadzu, Kyoto, Japan). Identification of flavonoids was carried out on the basis of diode array spectra, MS molecular ions, and MS/MS fragmentation patterns. Data obtained were compared with those available in scientific literature. Molecular formulae were calculated by the Formula Predictor software (Shimadzu).

3.3. Evaluation of the anti-oxidant capacity in *cell-free* models

3.3.1. Folin-Ciocalteu assay

The total phenolic content of BJe was determined by the Folin-Ciocalteu assay, following Tomaino et al. (2010). Briefly, 50 µL of methanol/water solutions of different sample concentrations were added to 450 µL of deionized water, 500 µL of Folin-Ciocalteu reagent, and 500 µL of 10% sodium carbonate solution and incubated in the dark at room temperature for 1 h, vortexing every 10 min. Absorbance was recorded at 786 nm (PrixmaUV-Vis Spectrophotometers) against a blank containing 50 µL of the same solvent used to dissolve the extracts. Total phenol content is expressed in mg of gallic acid equivalents (GAE/g of dried extract).

3.3.2. Quenching of the stable 2,2-Diphenylpicrylhydrazyl (DPPH) Radical assay

The DPPH assay was used to evaluate the radical scavenging activity of BJe. Following the procedure devised by Tomaino et al. (2010), different concentrations (ranging from 0.1 to 1 mg/mL) of methanol/water solution of each extract or vehicle alone (37.5 µL) were added to 1.5 mL of DPPH methanolic solution (25 mg/L). Absorbance was measured at 517 nm 30 min after starting the reaction. Free radical scavenging capacity of juice extracts is expressed in mg of Trolox equivalents (TE/g of dried extract).

3.3.3. Oxygen radical absorbance capacity (ORAC) assay

Antioxidant activity of BJe against 2,2'-azobis (2-amidinopropane) dihydrochloride (AAPH) peroxyl radicals was chemically examined using the ORAC method described by

Dávalos et al. (2004) with some modifications. Briefly, several concentrations of BJe (20 µL) in 75 mM phosphate buffer solution (pH 7.4) were mixed with 120 µL of 417 nM fluorescein solution and incubated at 37°C for 15 min to which 60 µL of AAPH (40 mM) was then added. Fluorescence was recorded spectrofluorometrically every 30 sec for 90 min (λex 485; λem 520; FLUOstar Omega, BMG Labtech), and phosphate buffer instead of sample, and calibration solutions of Trolox (10-100 µM) were also included in each assay. The ORAC value was calculated using the area under the fluorescence decay curves and is expressed in µmoles of TE/g of dried extract.

3.3.4. Reducing power assay

The reducing power of BJe was determined following the method described by Martorana et al. (2013). In brief, 0.2 mL of several concentrations of extract were mixed with 0.5 mL of 0.2 M sodium phosphate buffer (pH 6.6) and 0.5 mL of 1% $K_3Fe(CN)_6$ and then incubated in a water bath at 50°C for 20 min. Subsequently, 0.5 mL of 10% TCA was added to the mixture which was centrifuged at 8300 ×g for 10 min. The supernatant (0.5 mL) was then mixed with 0.5 mL of distilled water and 0.1 mL of 0.1% ferric chloride solution and absorbance measured at 700 nm. Increased absorbance of the reaction mixture indicated increased reducing power. Ascorbic acid was used as a reference. Phosphate buffer was used as blank solution. Reducing power is expressed in mg of ascorbic acid equivalent (AAE)/g of dried extract.

3.4. Evaluation of the anti-oxidant activity of BJe in *in vitro* models

3.4.1. Cell culture and treatment

The experiments were performed using a basal epithelial cell line A549 derived from human lung carcinoma (ATCC, Rockville, MD, USA). Cells were grown in 6-well plates (3×10^5 cells/well) and cultured in RPMI medium with 2 mM L-glutamine (Gibco Invitrogen, Milan, Italy), 10% (v/v) foetal bovine serum (FBS), 100 $IUmL^{-1}$ penicillin, and 100 gmL^{-1} streptomycin at 37°C in a humidified 5% CO_2 atmosphere. When 80–90% confluence was reached, monolayers were used for experiments by adding BJe to obtain a final concentration of 25 and 50 μgmL^{-1} in cell medium with 2% FBS. After 18 h, the medium was removed, and cells were washed and exposed to 200 µM H_2O_2 in PBS solution (pH 7.4) containing 10 mM D-glucose for further 2 h.

For each set of experiments, a negative control (untreated cultures) and a stressor control (H_2O_2 alone) were prepared by replacing the extract with PBS.

3.4.2. Cytofluorimetric analyses

Fluorescence-activated cell sorting (FACS) techniques were employed to determine the following parameters: intracellular ROS, lipid hydroperoxides, 8-oxo-7,8-dihydro-2'-deoxyguanosine (8-oxo-dG), transmembrane mitochondrial potential ($\Delta_{\psi m}$) and cell viability. After each experiment, the cells were harvested, centrifuged at 1000 ×g for 5 min, washed and suspended in PBS. Aliquots of cell suspensions ($\sim2\times10^5$ cells mL^{-1}) were used for each probe as described below. The data collected from each probe were used to draw the respective curves by calculating the average of cell percentages for each emission value. In FACS analyses, the weighted average of emission values per

100 cells was calculated and is expressed in arbitrary fluorescence units (AFU). The values obtained were used to calculate the percentage changes (%Δ) compared to the respective control.

3.4.2.1. DCF-DA staining assay

To determine intracellular ROS accumulation, cells suspensions were incubated for 30 min at 37°C with 1 µM 2-7-dichlorofluorescein diacetate (DCF-DA) probe. DCF-DA was deacetylated intracellularly by non-specific esterase and then oxidized by ROS to the fluorescent compound 2'-7'-dichlorofluorescein (DCF). Fluorescence emitted by DCF in FL-1 channel was detected by a Dako Galaxy flow cytometer (Dako Galaxy Cytomation).

3.4.2.2. DPP staining assay

Lipid hydroperoxides were detected using the diphenyl-1-pyrenylphosphine probe (DPPP; Invitrogen Molecular Probe, Milan, Italy) as reported by Di Pietro et al., (2009). The probe reacts stechiometrically with lipid hydroperoxides in cell membranes to yield a fluorescent phosphine oxide (DPPP=O) and the corresponding hydroxide. DPPP was added to cell suspensions to obtain a final concentration of 150 µM and incubated at 37°C for 3 h. Fluorescent phosphine oxide signals were then collected in the FL-1 channel.

3.4.2.3. R123 staining assay

Change in $\Delta\psi$m as result of mitochondrial perturbation, was evaluated by measuring the incorporation of rhodamine 123 (R123; Invitrogen, Life Technologies), which can

cross the mitochondrial membrane and to accumulate in the matrix of functional mitochondria. The fluorochrome (R123 0.2 μM) was added to cells suspension and incubated at 37°C for 10 min. The emitted fluorescence was then collected in the FL-2 channel.

3.4.2.4. 8-oxo-dG assay

Although all DNA bases are susceptible to damage, guanine is the most prone to oxidative modification. Eight-hydroxyguanine (8-OH-Gua) and its 2'-deoxynucleoside equivalent, 8-hydroxy-2'-deoxyguanosine (8-oxo-dG), are the most common byproducts. The latter is removed during the repair of damaged DNA by exonucleases as it is considered a marker of oxidant-induced DNA damage (Caramori et al., 2011). The level of 8-oxo-dG was estimated by FITC-labelled avidin probe which binds to 8-oxo-dG with high specificity due to the structural analogies between the keto form of the oxidized base and biotin. The method, previously adapted to flow cytofluorimetric analysis (Di Pietro et al., 2011), was performed in cells permeabilized by methanol (15 min at -20°C) and loaded with the avidin-FITC conjugate (1 h at 37°C). The emission signals were collected in FL-1 channel.

3.4.2.5. PI supravital staining assay

For PI staining, at the end of the treatments, supernatants were collected, the cells were detached with trypsin and pooled with corresponding supernatants. Cells were washed in PBS and stained with PI (3 $\mu g mL^{-1}$) at 4°C for 3 min. Dead cells, stained with the DNA intercalating probe, were cytofluorimetrically counted measuring the

emission signals in the FL-3 channel. Percentage of dead cells was calculated versus non-treated cells.

3.4.3. Comet assay

In order to examine the DNA integrity (potential genotoxic effect) in cells treated with the BJe, the alkaline version of comet assay was performed as reported (Picerno et al., 2006). Briefly, at the end of each treatment, cells were collected, washed with ice-cold PBS and 10 µl of cell-suspension ($1x10^6$ cells/ml) were dissolved in Low Melting Point (LMP) Agarose and spread on pre-coated-agarose microscope slides. The cells were lysed and then placed in a horizontal electrophoresis box. Subsequently, the cells were exposed to alkaline condition for 20 min to allow DNA unwinding and expression of alkali-labile sites. To electrophorese the DNA, an electric current of 25 V (0.86 V/cm) and 300 mA was applied for 30 min. Then, the slides were neutralized, stained with ethidium bromide (20 μgmL^{-1}) and analyzed using DM IRB fluorescence microscope at 400X magnification (Leica Microsystems Heidelberg, Mannhei, Germany), equipped with a digital camera (Canon Power Shot S50, Milan, Italy). For each coded spot, images of at least 100 randomly-selected nuclei were acquired and submitted to the Comet Assay Software Project (CASP) Lab automated image analysis system (http://www.casp.sourceforge.net). The following parameters were considered: tail length (TL), percentage of DNA in the head (HDNA %), percentage of DNA in the tail (TDNA %), tail moment (TM) and olive tail moment (OTM).

3.4.4. ROS and $\Delta_{\psi m}$ determinations by confocal microscopy observations

A549 cells were grown on cell chamber slides and treated as described above. The two probes DCF-DA and R123 were used separately to load cells. Treated and untreated cells were observed using TCS-SP2 confocal laser scanning microscopy (CLSM) equipped with an Ar/Kr laser (Leica Microsystems, Germany).

3.4.5. Statistical analysis

All data presented in the section 4.3 are shown as mean ± S.E.M. of at least three independent experiments. Significance was set at P<0.05. Comparisons and correlations were calculated using one-way analysis of variance (ANOVA) and Pearson's correlation coefficient, respectively.

3.5. Evaluation of the chelating property of BJe in *in vitro* models

3.5.1. Cell culture and treatment

The experiments were assessed on the A549 cells line (ATCC, Rockville, MD, USA). Cells were cultured as described in paragraph 3.4.1.

To assay the capacity of BJe to protect A549 cells from iron-mediated oxidative injury, cells were pre-incubated for 18 h in presence of different concentrations of the extract, directly diluted in cell medium with 2% FBS. At the end of the pre-incubation time, the medium was changed before the addition of the metal solutions (200 µM or 400 µM of $Fe_2(SO_4)_3$ for 2 h). Considering the intracellular presence of iron chelators, as in particular citrate and ATP, apparently high iron concentrations were used. Following controls were included for each experiment: (i) A549 cells without any treatment to evaluate the basal oxidative status; (ii) A549 cells not-treated with BJe and exposed to 200 or 400 µM Fe^{3+} as positive control; (iii) A549 cells treated with BJe and no-exposed to iron to assess the effect of extract in the basal condition.

3.5.2. Cell viability assay

Cell viability in presence of BJe was determined by the 3-(4,5-dimethylthiazole-2-yl)-2,5-diphenyltetrazolium bromide (MTT) test. A549 cells were seeded onto 96-well plates (10×10^3cells/well). Twenty-four hours after plating, the growth medium was replaced with fresh medium (untreated cells) or with medium supplemented with increased dilution of BJe ranging from 0 to 2500 µg mL^{-1}. After 24 h the plates were centrifuged and the supernatant was replaced with 100 µL of fresh media without red phenol, containing 0.5 mg mL^{-1} of MTT. Four hours later, crystals of formazan were

solubilized by HCl/isopropanol 0.1 N buffer and quantified at a wavelength of 570 nm (reference at 690 nm) with a microplate spectrophotometer (Tecan Italia, Cologno Monzese, Italy). Results were expressed as percentages of MTT reduction in comparison to untreated cultures.

3.5.3. Analyses of oxidative stress markers

FACS analyses (Novocyte 2000, ACEA Bioscences Inc., San Diego, California, USA) were performed to determine the following parameters: intracellular ROS, lipid hydroperoxides, 8-oxo-dG and $\Delta_{\psi m}$.

Cells were grown in 6-well plates (5×10^5 cells/well) and treated as reported above. After each experiment, the cells were harvested, centrifuged at 1000 g for 5 min, washed and suspended in PBS. Aliquots of cell suspensions ($\sim 2 \times 10^5$ cells mL^{-1}) were used for each probes. FACS analyses were performed as described above (see paragraphs 3.4.2.1 for ROS, 3.4.2.2 for lipid hydroperoxides, 3.4.2.4 for 8-oxo-dG and 3.4.2.3 for $\Delta_{\psi m}$). FACS analyses were performed in triplicate and the weighted average of emission values for 100 cells was calculated and expressed in arbitrary fluorescence units (AFU).

3.5.4. Comet assay

Cells treated as reported in paragraph 3.5.1. were assayed for DNA integrity by the alkaline version of comet assay (for method see paragraph 3.4.3).

3.5.5. Analysis of intracellular free iron

The chelating property of BJe was assessed using the calcein-acetoxymethyl ester (calcein-AM) as probe. Calcein-AM is a non-fluorescent non-chelating lipophilic ester that easily penetrates cellular membranes and diffuses in the cells. Here, it is rapidly cleaved by unspecific cytosolic esterases producing the fluorochromic alcohol calcein (λex 488 nm; λem 518 nm), that chelates intracellular free iron (Cabantchik, 2014). This reaction quenches the green fluorescence of calceinin in a concentration dependent manner, allowing the detection of uncomplexed iron. In order to validate the assay, performed to assess the presence of redox active iron in an *in vitro* model, deferiprone (DFP 0.3 M) was used as positive control. This well-tested drug, widely used in the therapy of siderosis, is a bidentate ligand fat-soluble and therefore capable to complexing intracellular iron. Briefly, cell suspensions ($1 \times 10^5\ mL^{-1}$), treated as above reported, were loaded with calcein-AM (final concentration 60 nM). Cell suspensions were incubated a 37°C for 15 min and then submitted to FACS analysis collecting signals in the fluorescence channel 1.

3.5.6. Fluorimetric abiotic assay

The chelating property of BJe was confirmed by using a fluorimetric abiotic assay, based on the method devised by Esposito et al. (2003). Briefly, we measured in Fe^{3+} solutions, prepared both in PBS and in BJe solutions, the oxidation of the non-fluorescent probe dihydrorhodamine (DHR) to its fluorescent form rhodamine, due to redox-active iron (uncomplexed). Analyses were performed in triplicate in 96-well plates adding the DHR (50 µM) in reagent solution (pH 7.3) containing 40 µM of ascorbate to form Fe^{2+} from Fe^{3+}. Emitted fluorescence was recorded every 2 min

starting from 15 min up to 40 min using a multiwall plate reader with excitation/emission filters of 485/538 nm (Tecan, Brescia, Italia). The difference between Fe in PBS solution and in BJe solution was used to assess chelating activity. DFP was used as positive control.

3.5.7. Enzymatic activity and mRNA level of the anti-oxidant catalase enzyme

The indirect antioxidant effects of BJe, due to enhanced expression of defense genes, were evaluated by measuring both mRNA level and enzymatic activity of the antioxidant catalase enzyme. Cells were grown in 6-well plates (5×10^5 cells/well) and treated as reported above. At the end of the treatments, the cells were detached with trypsin and pooled with supernatants.

For catalase activity a commercial kit from AbCam (Cambridge, UK) was used following the protocol recommended by the manufacturer. The obtained results, are reported as percentages of catalase activity in comparison to untreated cultures. Expression of mRNA was assessed by real-time PCR. Total RNA from cells was extracted using TRIzol reagent according to the manufacturer's protocol. Then, equal amounts of total RNA (2 µg) were reverse transcribed using High-Capacity cDNA Archive Kit (Applied Biosystems, Foster City, CA). Quantitative PCR reactions were set up in triplicate in a 96-well plate and were carried out in 20 µL reactions containing 1x SYBR® SelectMaster Mix (Applied Biosystems), 0.1 µM of following primers for catalase (forward 5'-TGGACAAGTACAATGCTGAG-3' and reverse 5'-TTACACGGATGAACGCTAAG-3'), and 25 ng RNA converted into cDNA. β-Actin was used as housekeeping control. Data were collected and analyzed using the $2^{-\Delta\Delta CT}$ relative quantification method.

3.5.8. Statistical analysis

All data presented in the section 4.4 are shown as mean ± S.E.M. based on at least three independent experiments. Data were analyzed by one-way analysis of variance (ANOVA). Multiple comparisons of the means of the group were performed by the Tukey-Kramer test (GrafPAD Soft-ware for Science). Significance was accepted at $P<0.05$.

3.6. Assessment of the anti-inflammatory effect of BJe against LPS in an *in vitro* model

3.6.1. Cell culture and treatment

The human leukemia monocytic cell line, THP-1, was purchased from American Type Culture Collections (ATCC) (Rockville, MD, USA). THP-1 cells were maintained in RPMI 1640 supplemented with L-glutamine (2 mM), HEPES (10 mM), sodium pyruvate (1 mM), glucose (2.5 g/l), 2-mercaptoethanol (0,05 mM), 10% heat-inactivated fetal bovine serum (FBS), 1% penicillin/streptomycin, at 37°C in a 5% CO_2/95% air humidified atmosphere. All reagents for cell culture were from Sigma (Milan, Italy).

Medium was renewed every 2 days and split performed when cells reached maximum density ($1x10^6$ cells/ml). In our experimental conditions, THP-1 cells were seeded at a density of $5x10^5$ cells/ml into culture plates in RPMI complete medium plus 10% FBS and incubated at 37°C with 500 ng/ml of lipopolysaccharide (LPS; InvivoGen, San Diego, CA, USA) for 3 h, in the presence or absence of BJe (0.05-0.1-0.5 mg/ml) and/or Sirtinol (1-5-10 μM; Sigma), which were added to the culture medium 30 min prior to LPS treatment. In all experiments, equal volumes of PBS or DMSO were added to the medium of control cultures (controls were performed using non-stimulated cell).

The concentrations of LPS, BJe and Sirtinol were chosen according to our preliminary optimization studies. After incubation, cells were harvested by centrifugation to assess cellular viability, gene expression, activation of transcription factor NF-kB and acetylation status of p65. Media were collected in order to evaluate cytokines release.

3.6.2. Cell viability assay

To assess both LPS and BJe cytotoxicity, we evaluated the mitochondrial activity of living cells by a MTT quantitative colorimetric assay. After treatment, THP-1 cells were harvested by centrifugation and, after counting, they were incubated in 96-well culture plates at a density of $5x10^4$ cells/well with fresh red-phenol free medium containing MTT (0.5 mg/mL; Sigma) at 37°C for 4 h. Then, insoluble formazan crystals were dissolved in 100 mL of a 0.04 N HCl/isopropanol solution for 1 h. The optical density in each well was evaluated by spectrophotometrical measurement. Absorbance was determined at 570 nm using a microplate reader (Tecan Italia, Cologno Monzese, Italy). All experiments were performed in eightplicate and repeated three times.

3.6.3. Real-Time PCR

After RNA isolation with TRIzol reagent, RNA (3 μg) was reverse transcribed with High-Capacity cDNA Archive kit according to the manufacturer's instructions. Then, mRNA levels of IL-6, IL-1β, TNF-α were analyzed by real-time PCR using TaqMan gene expression assays according to the manufacturer's instructions. 18S mRNA was used as endogenous controls.

Quantitative PCR reactions were set up in triplicate in a 96-well plate and were carried out in 10 μl reactions containing 1x TaqMan Gene Expression Mastermix, 1x TaqMan-specific assay and 20 ng RNA converted into cDNA. qPCR was performed in a 7900HT Fast Real-Time PCR System with the following profile: one cycle at 50°C for 2 min, then 95°C for 10 min, followed by 50 cycles at 95°C for 15 s and 60°C for 1 min. Data were collected and analyzed using SDS 2.3 and RQ manager 1.2 software (Applied

Biosystems, Foster City, CA) using the $2^{-\Delta\Delta CT}$ relative quantification method. Values are presented as fold change relative to unstimulated cells.

3.6.4. Evaluation of cytokine secretion by ELISA

In order to detect human IL-6, IL-1β and TNF-α, an enzyme linked immunosorbent assay was performed in *cell-free* culture supernatants of THP-1 monocytes, using Instant ELISA Kits. Before detection, supernatants recovered from treated and untreated cells were concentrated 10-fold by freeze-drying. All freeze-dried samples were reconstituted by the addition of distilled water. Briefly, according to the manufacturer's guidelines, 50 µl of standards or samples (supernatants recovered from treated and untreated cells) were incubated in 96-well plates at room temperature for 3 h with shaking. After washing 5 times with 400 µl of wash buffer, 100 µl of the provided substrate solution were added to each well and the plates were incubated in the dark for 10 min. The enzyme reaction was then stopped by pipetting 100 µl of stop solution into each well and the absorbance was determined at 450 nm using a microplate reader (Tecan, Italy). All experiments were performed in triplicate.

3.6.5. Electrophoretic mobility shift assay

At the end of the treatment, THP-1 cells were harvested by centrifugation. After washing twice with cold PBS, the isolation of nuclear cell proteins was performed using a commercial nuclear extraction kit following the manufacturer's guidelines. Protein concentrations were determined using a Bradford method. The presence of NF-κB DNA binding activity in cellular nuclear extracts of LPS-treated and control cells was evaluated by subsequent electrophoretic mobility shift assay, using Affymetrix EMSA

Kits according to the manufacturer's instructions. Briefly, nuclear extracts were incubated with the biotin-labeled NF-κB probe and then the protein/DNA complexes were separated on a non-denaturing 6% polyacrylamide gel. After transferring onto nylon membranes bound complexes were detected via streptavidin-HRP and a chemiluminescent substrate and visualized on Kodak film. The bands were scanned and quantified by densiometric analysis with ImageJ 1.47, an open source software freely downloadable from the US National Institute of Health website (http://imagej.nih.gov/ij/).

3.6.6. Immunoprecipitation and immunoblotting analyses

For each sample, 50 µg of nuclear extract were incubated with rabbit anti-p65 for 1 h at 4°C on a rotator. Negative control was set by incubating nuclear proteins under similar conditions but without the immunoprecipitating antibody. Afterwards, 35 µl of re-suspended Protein G PLUS-Agarose beads were added to each tube and the samples were incubated at 4°C overnight on a rocker platform. The agarose beads were extensively washed the next day and pellets were re-suspended in 40 µl of 1x Laemmli buffer, boiled for 5 min and resolved by SDS-PAGE. Proteins were then transferred onto nitrocellulose membrane and non-specific binding sites were pre-blocked by incubation with 5% non-fat dry milk in Tris-buffered saline containing 0.15% Tween 20 for 1 h at room temperature. The blot was probed overnight at 4°C with primary antibody anti-acetylated Lysine (from sheep, diluted 1:1000), followed by incubation for 2 h with horseradish peroxidase conjugated anti-sheep secondary antibody (diluted 1:3000). Final detection was performed by using ECL chemiluminescence system; then, bands were scanned and quantified by densitometric analysis with ImageJ software.

3.6.7. Statistical analysis

Data of the section 4.5. were obtained from three separate set of experiments and were expressed as mean ± S.E.M. They were analyzed by the one-way analysis of variance (ANOVA) followed by the Student-Newman Keuls test using GraphPad Prism software (San Diego, CA). $P<0.05$ was considered significant.

3.7. Employment of an *in vitro* model to assess the capability of BJe to prevent the neuro-inflammatory action of β-amyloid

3.7.1. Cell culture and treatment

THP-1 cells were cultured as described in paragraph 2.6.1. Before use, $A\beta_{1-42}$ was dissolved in DMSO and kept at 37°C for 7 days to allow fibril formation as previously described by Giri et al. (2003). Fibril formation was checked according to the Congo red staining method described by Wang et al. (2005), which is based on measurements of absorbance/turbidity at 405 nm of the Aβ sample solution. The progressive increase of absorbance of Aβ solution was an indication of the degree of aggregation that increased with the progression of aggregation.

To evaluate the time-dependent effects of Aβ on cytokine mRNA levels, THP-1 cells were seeded at a density of 5×10^5 cells/ml into culture plates and incubated at 37°C with 0.5 μM fibrillar $A\beta_{1-42}$, in RPMI complete medium plus 2% FBS, up to 24 h.

In further experiments, THP-1 cells were incubated at 37°C with/without 0.5 μM fibrillar $A\beta_{1-42}$ for 16 h, in the presence or absence of either BJe (0.05, 0.1 and 0.5 mg/ml) or N-acetyl-L-cysteine (NAC; 500 μM), which were added to the culture medium 30 min prior to $A\beta_{1-42}$ treatment.

To ascertain the specificity of fibrillar $A\beta_{1-42}$ effects, in a subset of experiments soluble $A\beta_{1-42}$ ($sA\beta_{1-42}$), $A\beta_{42-1}$, and $A\beta_{1-40}$, at a concentration of 0.5 μM each, were tested as controls. In all experiments, equal volumes of DMSO or PBS were added to the medium of untreated control cultures. After incubation, cells were harvested by centrifugation to assess cytokine expression, cell viability, ROS production, protein

levels of MAPKs. Additionally, activation of transcription factors, such as NF-κB and AP-1, was evaluated. Media were collected in order to evaluate cytokines release.

3.7.2. Cell transfection using AP1 ODNs

Suspended THP-1 cells, seeded at a density of 5×10^5 cells/well into 24-well culture plates, were transfected with 1 μM double-stranded AP-1 ODN with Lipofectamine 2000, according to the manufacturer's instructions. After 24 h of incubation, cells were exposed to 0.5 μM $A\beta_{1-42}$ for further 16 h. Cells transfected either with mutant ODN or lipofectamine alone were used as internal negative control for transfection.

The sequences of the phosphorothioated and single-stranded decoy oligodeoxynucleotides (ODNs) were as follows: AP-1 ODN, 5'-CGCTTGATGACTCAGCCGGAA-3', 3'-GCGAACTACTGAGTCGGCCTT-5'; corresponding mutant ODN, 5'-CGCTTGATTACTTAGCCGGAA-3', 3'-GCGAACTAATGAATCGGCCTT-5'.

3.7.3. Analysis of cytokine expression and secretion

At the end of treatments, cells were harvested by centrifugation, and total RNA was isolated using TRIzol. Then, RNA (2 μg) was reverse transcribed with High-Capacity cDNA Archive kit according to the manufacturer's instructions. The mRNA levels of IL-6, IL-1β, and TNF-α were assessed by Real-time RT-PCR as described in paragraph 3.6.3.

Data were collected and analyzed using SDS 2.3 and RQ manager 1.2 software using the $2^{-\Delta\Delta CT}$ relative quantification method. Values are presented as fold change relative to control cells. In order to detect human IL-6 and IL-1β, an ELISA was performed in *cell-free* culture supernatants of THP-1 monocytes, using Instant ELISA Kits as described in paragraph 3.6.4.

3.7.4. Cell viability assays

To assess either $A\beta_{1-42}$ or BJe adverse effects on cell viability, we used both 3-(4, 5-Dimethylthiazol-2-yl)-5-(3-carboxymethoxyphenyl)-2-(4-sulfophenyl)-2H-tetrazolium (MTS; Promega, Milan, Italy) and PI exclusion assays.

THP-1 monocytes were seeded at a density of 5×10^4 cells/well in 100 µl/well of medium without phenol red onto 96-well plates. The next day, cells were exposed to 0.5 µM fibrillar $A\beta_{1-42}$ in presence or absence of 0.05 and 0.1 mg/ml BJe, added to the culture medium 30 min prior to $A\beta_{1-42}$. After 16 h of treatment, 20 µl/well MTS reagents was added into each well, and the plates were incubated at 37°C for 4 h in standard culture conditions. Then, the absorbance was recorded at 490 nm, by a microplate reader (Tecan Italia).

PI exclusion assay was carried out, as described by Lioi and co-workers (Lioi et al., 2012) with some modifications, in order to test both cytotoxicity and membrane integrity. Briefly, 5×10^5 cells were collected, re-suspended in 400 µl of PBS and incubated with 10 µl PI labeling solution for 20 min at room temperature in the dark. Cells were then analyzed with a NovoCyte 2000 flow cytometer (ACEA Bioscences).

A minimum of 10000 events were counted per sample.

3.7.5. Measurement of intracellular reactive oxygen species

The production of ROS was quantified by fluorescent staining with DCF-DA. At the end of treatments, cells were incubated with 5 µM DCF-DA for 30 min at 37 °C. After two washes with PBS (pH 7.4), cells were centrifuged and re-suspended in 500 µL of PBS supplemented with 0.1 M KH_2PO_4 and 0.5% Triton X-100. Cells debris were pelleted by

centrifugation at 2000 × g for 10 min, and the supernatants were analyzed under fluorescein optics, at an excitation wavelength of 480 nm and an emission wavelength of 540 nm. Cell lysates were analyzed for protein content using the Bradford method, and DCF fluorescence was normalized for total protein content.

3.7.6. Analysis of MAPK expression

After cell lysis by extraction kit, the cytosolic fraction of cell lysates was loaded at 30 µg per well and resolved by electrophoresis on a 10% SDS-PAGE gel. Then, proteins were transferred by electroblotting onto nitrocellulose membrane, and non-specific binding sites were pre-blocked by membrane incubation with 5% non-fat dry milk in Tris-buffered saline containing 0.15% Tween 20 (TBS-T) for 1 h at room temperature. The blots were probed overnight at 4°C with primary antibodies against total and phosphorylated JNK, ERK1/2, p38 (diluted 1:1000 in TBS-T) and β-actin (diluted 1:5000 in TBS-T); then, they were washed five times with TBS-T, and incubated for 2 h with HRP-conjugated anti-rabbit and anti-mouse secondary antibodies (diluted 1:3000 and 1:15000, respectively). After washing with TBS-T, final detection was performed by using ECL chemiluminescence system; then, bands were scanned and quantified by densitometric analysis with ImageJ.

3.7.7. Assessment of transcription factor activation

At the end of incubation, THP-1 cells were harvested by centrifugation. After washing twice with cold PBS, the isolation of nuclear cell proteins was performed using a Nuclear Extraction Kit, according to the manufacturer's guidelines. Protein concentration was determined by Bradford method. The presence of NF-κB DNA

binding activity in nuclear extracts of treated and control cells was evaluated by EMSA kit according to the manufacturer's instructions.

AP-1 binding activity was assessed by using the LightShift Chemiluminescent EMSA kit. Before analysis, the double-stranded AP-1 probe (21 bp) was biotin-end labeled by terminal deoxynucleotidyl transferase (TdT) included in the Biotin 3' End DNA Labeling kit. Nuclear proteins (2 μg) were incubated with the biotin-labeled NF-κB or AP-1 probes; then, the protein/DNA complexes were resolved by electrophoresis on a non-denaturing 6% polyacrylamide gel. After electroblotting onto a nylon membrane, detection of protein/DNA complexes was performed by chemiluminescence methods using streptavidin-HRP. Bands were scanned and quantified by densitometric analysis with ImageJ 1.47.

3.7.8. Statistical analysis

Data presented in the section 4.6. were obtained from three separate set of experiments and were expressed as mean ± S.E.M. They were analyzed by either Student's t test or one-way analysis of variance (ANOVA) followed by the post hoc Student-Newman-Keuls multiple comparisons test using GraphPad Prism software (San Diego, CA). The $P<0.05$ was considered significant.

4. RESULTS

4.1. Flavonoid composition of BJe

Figure 1 shows a representative chromatogram of BJe used in all studies presented in this PhD thesis. It was obtained by a UHPLC coupled online to an LCMSIT-TOF mass spectrometer. The peaks identify each compounds present in the extract. Their quantity is expressed as mg/g and listed in table 1, and their molecular structures are presented in figure 2.

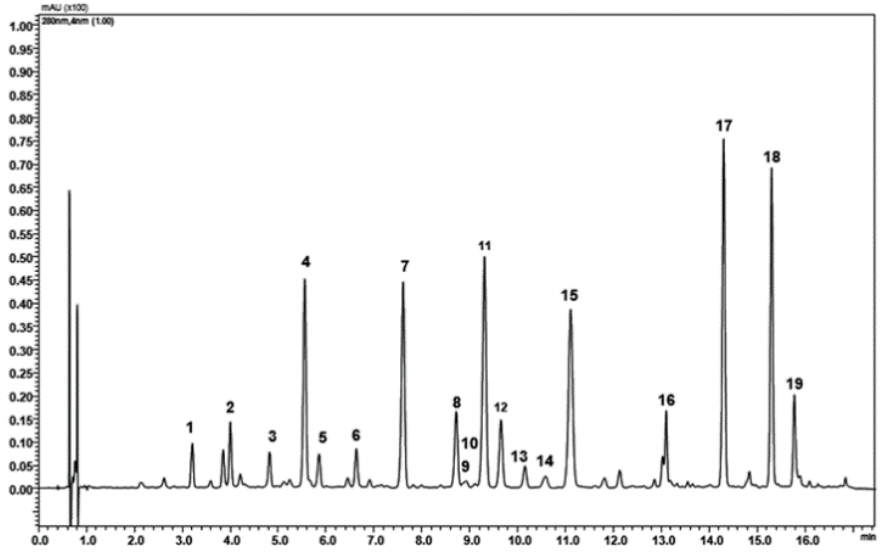

Fig. 1. UHPLC chromatogram of BJe.

The flavanones neohesperidin, naringin, hesperetin and neoeriocitrin are the molecules present in the highest amount. The flavones rhoifolin and neodiosmin are also abundant, while C-glucosidic compounds are in a minor quantity.

Interestingly, a relevant quantity of melitidin was found in the BJe used in this study.

peak	compounds	mg/g
1	Vicenin-2	11.61
2	Lucenin-2 4’-methyl ether	10.29
3	Eriocitrin	8.89
4	Neoeriocitrin	51.73
5	Poncirin	18.41
6	Orientin 4’ methylether	14.85
7	Naringin	91.90
8	Rhoifolin	19.96
9	Hesperidin	7.49
10	Isoquercitrin	2.5
11	Neohesperidin	98.5
12	Neodiosmin	12.39
13	Rhoifolin 4’-glucoside	2.55
14	Narirutin	4.97
15	Melitidin	79.47
16	Brutieridin	36
17	Naringenin	41.48
18	Hesperetin	53.84
19	Diosmetin	12.36

Tab. 1. Concentration of flavonoids in BJe expressed as mg/g.

FLAVANONE AGLYCONES

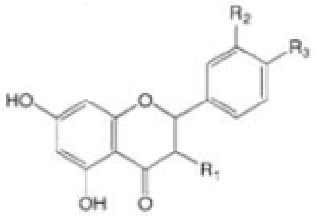

peak	compound	R1	R2	R3
17	Naringenin	H	H	OH
18	Hesperetin	H	OH	OMe

FLAVONE AGLYCONES

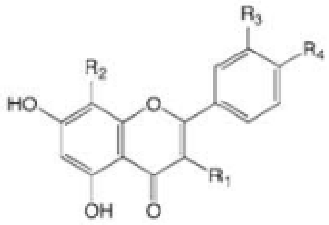

peak	compound	R1	R2	R3	R4
19	Diosmetin	H	H	OH	OMe

FLAVANONE - O - GLYCOSIDES

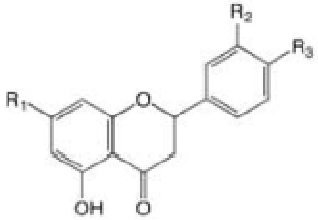

peak	compound	R1	R2	R3
3	Eriocitrin	O-Ru[a]	OH	OH
4	Neoeriocitrin	O-Nh[b]	OH	OH
5	Poncirin	O-Nh[b]	H	OMe
7	Naringin	O-Nh[b]	H	OH
9	Hesperidin	O-Ru[a]	OH	OMe
11	Neohesperidin	O-Nh[b]	OH	OMe
14	Narirutin	O-Ru[a]	H	OH
15	Melitidin	O-Nh[b]	H	OH
16	Brutieridin	O-Nh[b]	OH	OMe

FLAVONE - C - GLUCOSIDES AND FLAVONE - O - GLYCOSIDES

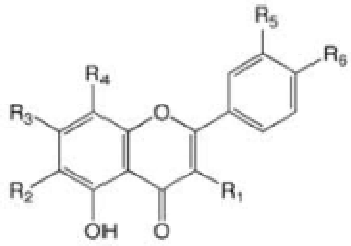

peak	compound	R1	R2	R3	R4	R5	R6
1	Vicenin-2	H	Glu	OH	Glu	H	OH
2	Lucenin-2,4'- methyl ether	H	Glu	OH	Glu	OH	OMe
6	Orientin 4' methyl ether	H	H	OH	Glu	OH	OMe
8	Rhoifolin	H	H	O-Nh[b]	H	OH	OH
12	Neodiosmin	H	H	O-Nh[b]	H	OH	OMe
13	Rhoifolin 4''- glucoside	H	H	O-Nh[b]	H	OH	O-Glu

Fig. 2. Chemical structures of flavonoids found in the BJe. [a]Rutinose (Ru); [b]Neohesperidose (Nh); Methyl group (Me); Glucoside (Glu).

In table 2, there are the amounts of single flavonoids (expressed as μg) present in the BJe at different concentrations (0.025, 0.05, 0.1 and 0.5 mg/ml) used in this study.

	BJe (mg/ml)			
Compounds	**0.025**	**0.05**	**0.1**	**0.5**
Vicenin-2	0.29	0.58	1.16	5.80
Lucenin-2 4'-methyl ether	0.25	0.51	1,02	5.14
Eriocitrin	0.22	0.44	0.88	4.44
Neoeriocitrin	1.29	2.58	5.17	25.86
Poncirin	0.46	0.92	1.84	9.20
Orientin 4' methylether	0.37	0.74	1.48	7.42
Naringin	2.29	4.59	9.19	45.95
Rhoifolin	0.49	0.99	1.99	9.98
Hesperidin	0.18	0.37	0.74	3.74
Isoquercitrin	0.06	0.12	0.25	1.25
Neohesperidin	2.46	4.92	9.85	49.25
Neodiosmin	0.30	0.61	1.23	6.19
Rhoifolin 4'-glucoside	0.06	0.12	0.25	1.27
Narirutin	0.12	0.24	0.49	2.48
Melitidin	1.98	3.97	7.94	39.73
Brutieridin	0.9	1.8	3.6	18
Naringenin	1.03	2.07	4.14	20.74
Hesperetin	1.34	2.69	5.38	26.92
Diosmetin	0.30	0.61	1.23	6.18

Tab. 2. Concentrations of flavonoids found in BJe at the indicated concentrations, expressed as μg.

4.2. Anti-oxidant capacity in *cell-free* models

The anti-oxidant and radical scavenging properties of BJe were determined using a series of chemical tests that results are shown in table 3.

ORAC µmol TE/g	8054.17 ± 606.11
DPPH mg TE/g	74.5 ± 10.8
Folin-Ciocalteu mg GAE/g	129.17 ± 2
Reducing power mg AAE/g	99.05 ± 2

Tab. 3. Anti-oxidant activity of BJe. Results are reported as mean ± S.E.M. of three experiments performed in triplicate and expressed as standard equivalent/g of dried extract.

4.3. Protective effect of BJe from H_2O_2-induced oxidative stress in A549 cells

4.3.1. BJe prevents the H_2O_2-induced increase of ROS

To study the potential protective effects of BJe in different compartments of oxidatively injured A549 lung epithelial cells, we first measured the intracellular content of ROS. As expected, DCF emission values in cells treated with BJe for 18 h did not differ significantly from the background values recorded in untreated cells (Fig. 3A). These results indicate that the extracts at both 25 and 50 μg/mL concentrations did not trigger ROS generation. Instead, DCF emission values in H_2O_2-stressed cells were up to 6.7-fold higher than those detected in untreated cultures, suggesting that there had been an increase in ROS generation (fig. 3A). Interestingly, as shown in fig. 3A, the presence of BJe reduced H_2O_2-induced oxidative stress, thus preventing the increase in ROS. Indeed, the fluorescence emission curve for untreated culture shows a consistent peak on the left of the graph (proportional to the number of cells with low emission values). In contrast, in A549 cells incubated with 200 μM H_2O_2 for 2 h a larger number of cells with high emission values was detected (the purple peak on the right), indicating an increased ROS production. The curves obtained from the cells pre-treated with BJe and then incubated with H_2O_2 show a smaller number of cells with high emission values. Figure 3B summarizes data from the cytofluorimetric analyses presented in figure 3A, showing the percentage of ROS reduction in A549 cells pretreated with BJe and then incubated with H_2O_2 in comparison to the cells exposed to H_2O_2 alone (%Δ). The histograms in fig 3B illustrate that BJe significantly reduced ROS production caused by H_2O_2 in A549 cells (P<0.01).

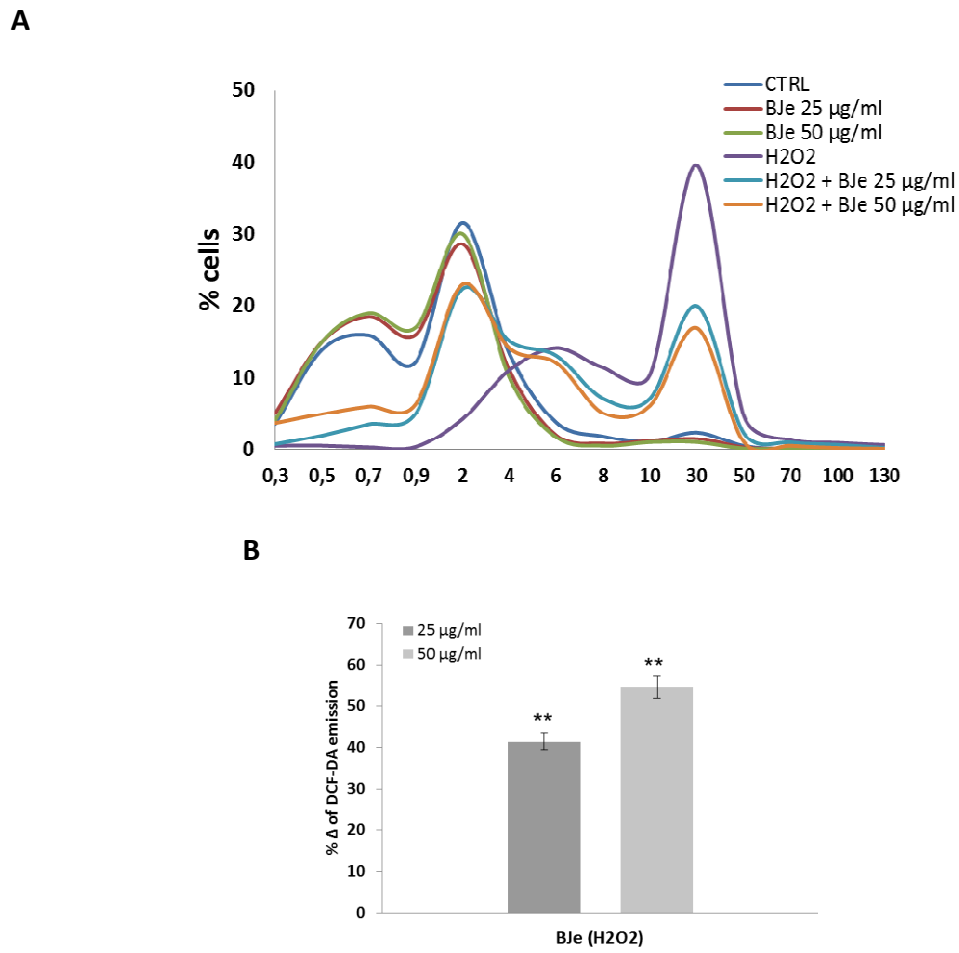

Fig. 3. Cytofluorimetric evaluation of intracellular ROS. A549 cells treated for 18 h with BJe were oxidatively stressed by H_2O_2 200 μM for additional 2 h. Results from BJe treatments (A). The curves shifted rightward to higher emission values indicate the increase of ROS production. Data from A are expressed as percentage of reduction (%Δ) of DCF-DA emission values in BJe-pretreated cells and then exposed to H_2O_2 compared to H_2O_2-stressed cells (B). The experiments were repeated at least three times. $**P<0.01$ *vs* H_2O_2-treated cells.

The data from FACS analyses were confirmed by CLSM observations. Figure 4 shows that, in comparison to oxidatively stressed A549 cells, the presence of BJe dampened the fluorescence emission proportionally to the concentration employed.

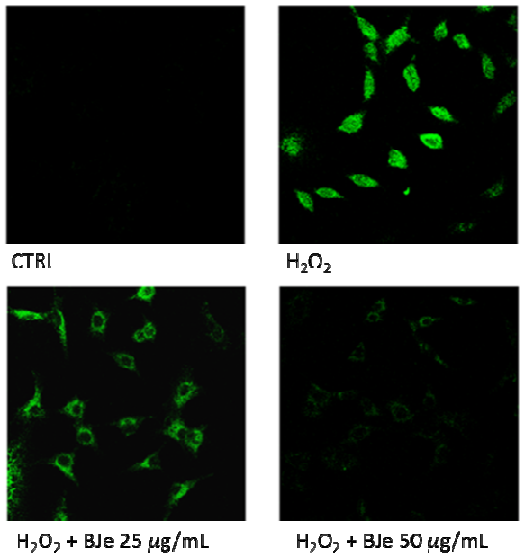

Fig. 4. Confocal laser scanning microscope images of DCF-DA-stained cells. A549 cells grown on cell slides were pre-incubated with BJe and after 18 h were exposed to H_2O_2 200 µM. Green fluorescence represented the amounts of ROS. Images shown are representative of three independent experiments. 400x magnification.

4.3.2. BJe reduces the H_2O_2- caused cell death

As shown in figure 5, no differences between cell exposed to BJe and then treated or untreated with H_2O_2 were recorded in PI emission values.

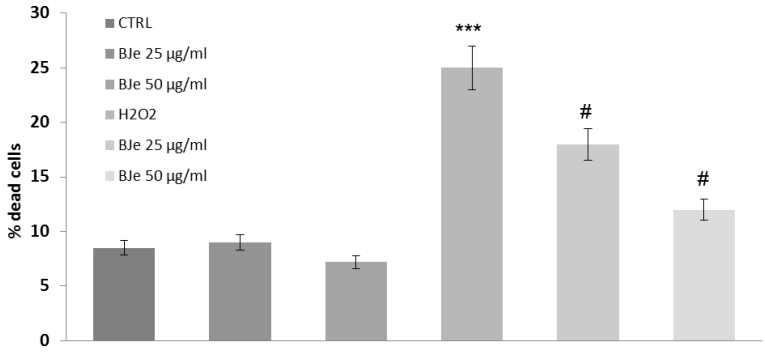

Fig. 5. Effect of BJe on cell death induced by H_2O_2. The cells were treated for 18 h with BJe followed by incubation with 200 µM H_2O_2 for additional 2 h. PI-positive cells were determined by flow cytometry collecting the emission signal in the FL-3 channel. Data represent means ± S.E.M. of three separate experiments. $^{***}P<0.001$ *vs* control cells and $^{\#}P<0.05$ *vs* H_2O_2-treated cells.

4.3.3. BJe counteracts lipid peroxidation induced by H_2O_2 in A549 cells

High lipid content of cell membranes makes them particularly susceptible to oxidative damage. Therefore we measured the lipid hydroperoxides to investigate the consequences of the oxidative damage caused by H_2O_2 on the membrane lipids and also to examine the effect of BJe. The level of lipid peroxidation in A549 cells increased up to 6-fold after 2 h incubation with 200 µM of H_2O_2, an effect counteracted by the pre-incubation with the extract (fig. 6). Interestingly, the DPPP emission value detected in H_2O_2-stressed cells were lowered by up to 40 and 55% by pretreatment with BJe at concentrations of 25 and 50 µg/mL, respectively (P<0.01).

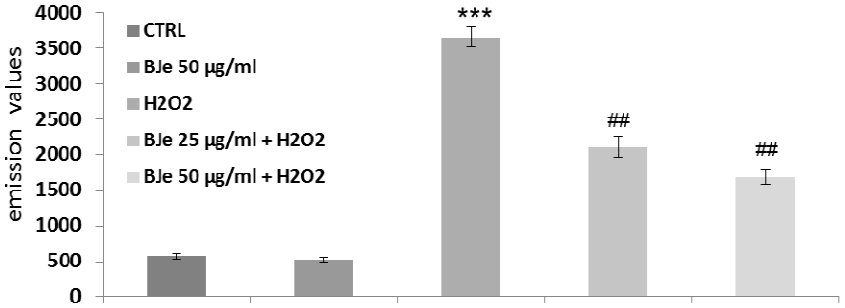

Fig. 6. Cytofluorimetric evaluation of lipid hydroperoxides. The A549 cells incubated for 18 h with BJe were oxidatively stressed with H_2O_2 200 µM for 2h and then loaded by DPPP probe. The graph reports the mean of fluorescence expressed in arbitrary fluorescence units (AFU) of three independent experiments. Data represent the mean ± SEM of at least three separate experiments. $^{***}P$<0.001 *vs* control cells and $^{\#\#}P$<0.01 *vs* H_2O_2-treated cells.

4.3.4. BJe attenuates the fall in $\Delta_{\psi m}$ induced by H_2O_2

Since mitochondrial membrane phospholipids are key targets for lipid peroxidation involving highly polyunsaturated side chains, we further evaluated the ability of BJe to restrain mitochondrial impairment. Figure 7 shows that incubation of A549 cells with H_2O_2 caused a drop in $\Delta_{\psi m}$, as indicated by the peak of the R123 probe fluorescence

emission on the left of the graph (fig. 7A). The presence of BJe lessened the ROS-induced mitochondrial impairment observed in stressed cells, reducing the number of cells with lower R123 fluorescence emission values. This is clearly shown in figure 7B which presents the increases in weighted-averages fluorescence found in cultures pre-incubated with BJe prior to H_2O_2 exposure, in comparison to the non-pretreated oxidatively stressed cells, set at 0 (P<0.05 and P<0.01 for 25 and 50 µg/mL of BJe, respectively).

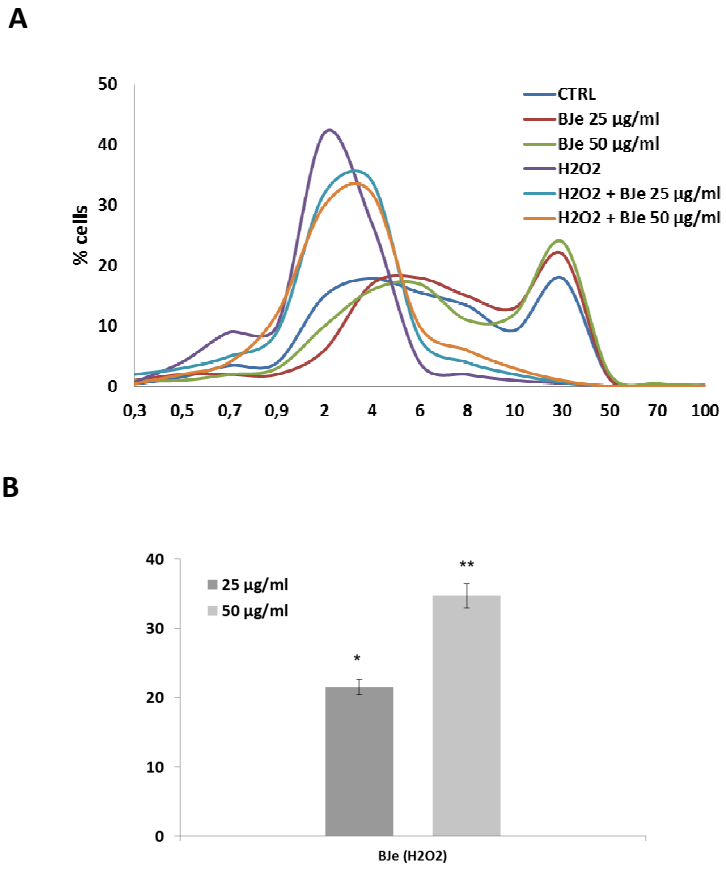

Fig. 7. Effect of BJe on mitochondrial membrane potential in H_2O_2-treated cells. The cells treated with BJe and then exposed to 200 M H_2O_2 for 2 h were loaded with R123 probe. Fluorescence was followed by flow cytometry. The shift of the curves to the left of the graph indicates the reduction of $\Delta\psi m$. Results from BJe exposure (A). In B are reported data from A expressed as percentage of increase of R123 emission values in BJe-pretreated cells subsequently exposed to H_2O_2 compared to H_2O_2-stressed cells (%Δ). $^{*}P$<0.05 and $^{**}P$<0.01 *vs* H_2O_2-treated cells.

The CLSM observations confirmed the results from FACS analyses, showing that the presence of BJe reduced the fall in $\Delta\psi$m, as revealed by the increased emitted fluorescence (fig. 8).

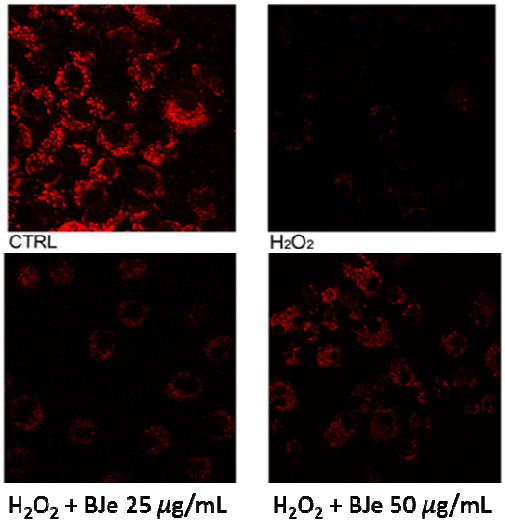

Fig. 8. CLSM analysis of mitochondrial membrane potential. A549 cells were grown on cell slides and after treatment with BJe were incubated with H_2O_2. Mitochondrial membrane potential was detected by R123 staining. Red fluorescence indicates functional mitochondria. Images captured at 400x magnification are shown as representative from three independent experiments.

4.3.5. BJe decreases oxidative DNA damage induced by H_2O_2

Levels of 8-oxo-dG and DNA strand breaks were measured to study the effectiveness of BJe to restrain DNA-oxidative damage. The results of cytofluorimetric analysis using a FITC-labelled avidin probe are reported in figure 9A. This shows that 18 h of treatment with BJe did not induce DNA oxidation since the emission values roughly overlapped those recorded in control cells. Despite the massive DNA damage induced by 2 h of H_2O_2 200 µM incubation, the pretreatment with BJe significantly decreased oxidative DNA damage by about 1.5 fold (P<0.01). Similar results were obtained using the comet assay (fig. 9B).

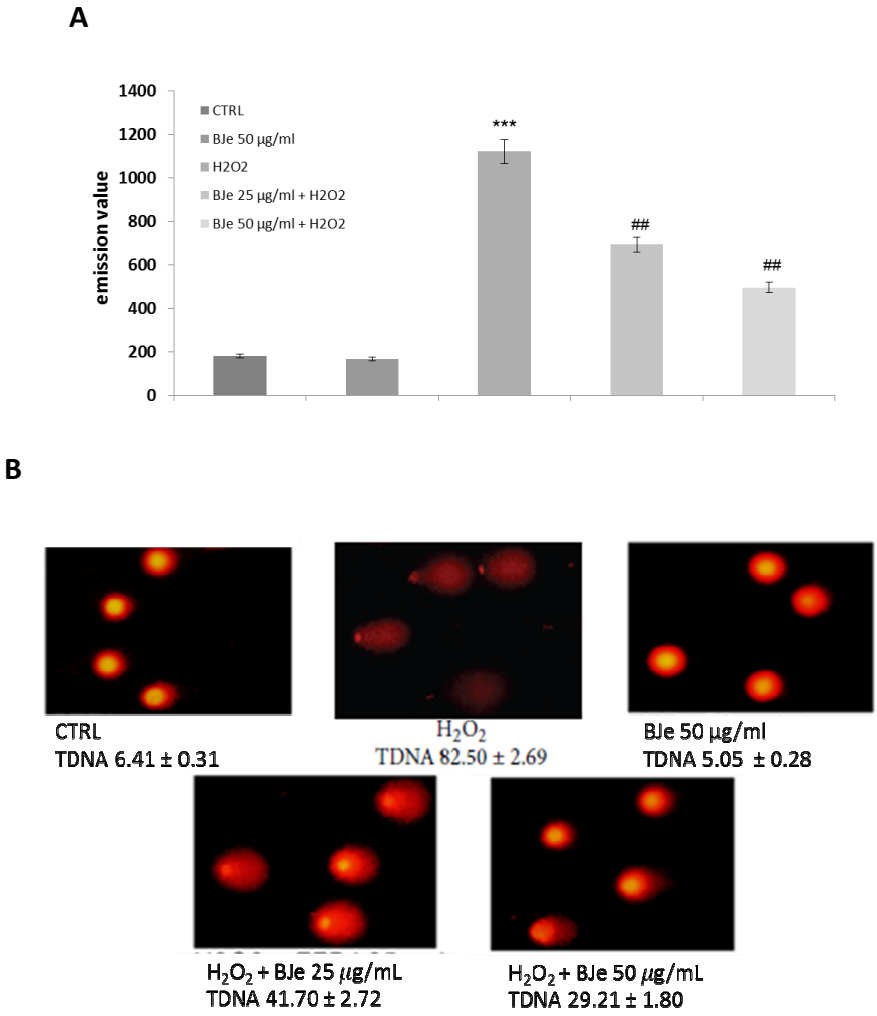

Fig. 9. Protective effects of BJe on DNA damage induced by H_2O_2. (A) Levels of 8-oxo-dG are measured as emission signals of fluorochrome FITC-labeled avidin collected in the FL-1 channel. The graph reports the mean of fluorescence expressed in arbitrary fluorescence units (AFU) of three independent experiments. $^{***}P<0.001$ *vs* control cultures and $^{\#\#}P<0.01$ *vs* H_2O_2-treated cells. (B) Images of comet assay captured by fluorescence microscopy at a magnification of 400x. A representative experiment that was replicated three times with similar results is shown. Percentages of tail DNA (TDNA) are indicated.

4.4. Protective role of BJe in Fe^{3+}-induced oxidative stress in A549 cells

4.4.1. Effects of BJe on cell viability in presence of Fe^{3+}

To further evaluate the effect of BJe extracts on the viability of A549 cells we performed the MTT test. BJe was assayed in the concentrations ranging from 0 to 2500 μg mL^{-1} and the results are reported in figure 10. The curve clearly shows the biphasic behavior of BJe in relation to its concentration. At the higher concentrations (≥1000 μg mL^{-1}) cytotoxic effect was observed and cell viability was significantly reduced (P<0.01). Instead, concentrations ≤500 μg mL^{-1} of BJe maintained cell viability roughly equal or slightly higher than untreated cells, suggesting a possible protective effect. We chose 25 and 50 μg mL^{-1} concentration to assess the BJe ability to counteract the iron-induced damage.

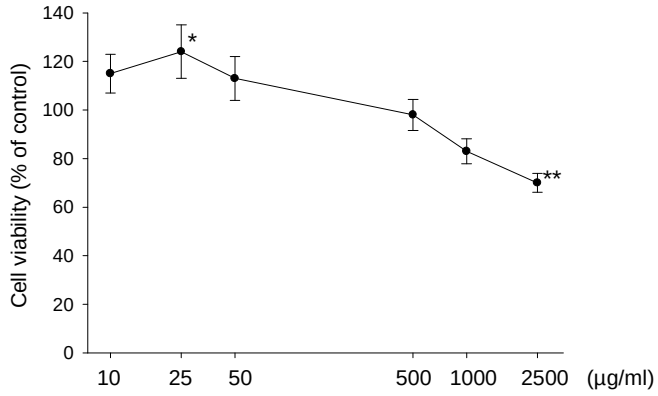

Fig. 10. Effect of BJe on cell viability. The cells were treated for 24 h with increasing concentration of BJe. Data of MTT assay are reported as means ± S.E.M. of three separate experiments performed in eigthplicate. *P<0.05 and **P<0.01 *vs* untreated cells.

4.4.2. BJe reduces the Fe^{3+}-induced increase of ROS

As shown in figure 11 compared with untreated cells, in 200 and 400 µM-iron treated A549 cells ROS levels increased up to 6 and 13-fold, respectively. The pre-treatment with BJe, was able to provide important protection against the Fe-induced ROS overproduction. In particular, based on the concentrations of $Fe_2(SO_4)_3$, BJe reduced ROS production in stressed cells between 50 and 70% at 25 or 50 µg mL^{-1} (P<0.001; fig. 11).

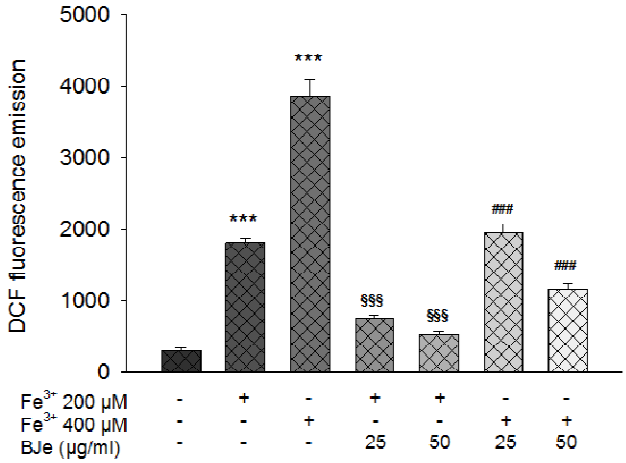

Fig. 11. Cytofluorimetric evaluation of intracellular ROS. A549 cells treated for 18 h with BJe were oxidatively stressed by Fe^{3+} 200 or 400 µM for additional 2 h. Cell suspensions were incubated with DCFH-DA 1 µM at 37◦C for 30 min. Fluorescent signals of DCF were collected in the FL-1 channel (530 ± 20 nm). The experiments were repeated at least three times. ***P<0.001 *vs* control cells; §§§P<0.001 *vs* Fe^{3+} 200 µM-treated cells; ###P<0.001 *vs* Fe^{3+} 400 µM-treated cells.

4.4.3. BJe counteracts lipid peroxidation induced by Fe^{3+}

The oxidative insult elicited by iron significantly affected membrane integrity, increasing the DPPP emission in cells treated with $Fe_2(SO_4)_3$ 200 and 400 µM up to 5.3 and 13-fold, respectively (fig. 12). Notably, the pretreatment with BJe, counteracted lipid peroxidation from 57 to 73% (P<0.001; fig. 12).

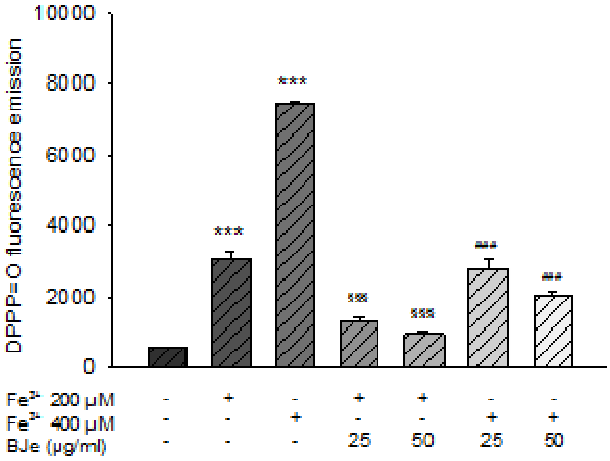

Fig. 12. Evaluation of lipid hydroperoxides. The A549 cells were exposed for 18 h with BJe and then treated with Fe^{3+} 200 or 400 µM for additional 2 h. Lipid hydroperoxides were citofluorimetric measured using DPPP (150 µM). The cells were incubated at 37°C for 3 h, then fluorescent signals were collected in the FL-1 channel. The experiments were repeated at least three times. ***P<0.001 *vs* control cells; $^{§§§}P$<0.001 *vs* Fe^{3+} 200 µM-treated cells; $^{###}P$<0.001 *vs* Fe^{3+} 400 µM-treated cells.

4.4.4. BJe reduces the fall in $\Delta_{\psi m}$ caused by Fe^{3+}

Exposure of A549 cells to $Fe_2(SO_4)_3$ caused a drastic drop of $\Delta_{\psi m}$ (about 50% and more than 75% in cells treated with 200 and 400 µM respectively; P<0.001) that only in part was mitigated by a pre-treatment with BJe. Indeed, the extract was able to improve the mitochondrial impairment caused by Fe^{3+} only when the stressor was used at the lower concentration (200 µM), increasing the transmembrane potential up to 30%. On the contrary, the protective effect exerted by BJe was negligible at 400 µM of $Fe_2(SO_4)_3$.

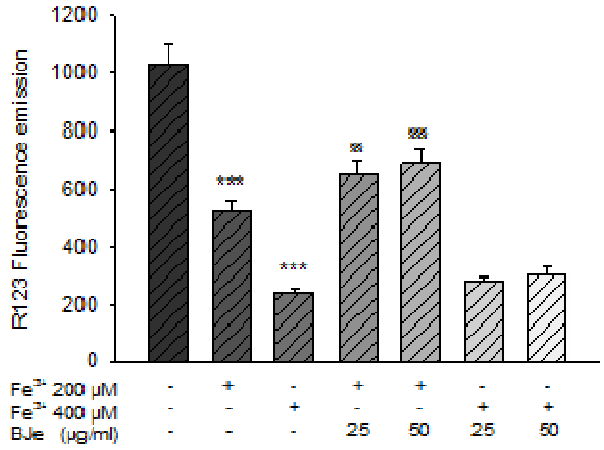

Fig. 13. Cytofluorimetric evaluation of mitochondrial membrane potential. A549 cells treated for 18 h with BJe were exposed to Fe^{3+} 200 or 400 µM for additional 2 h. The fluorescent probe R123 was used to evaluate the $\Delta_{\psi m}$. The fluorochrome was added to cell suspensions to a final concentration of 10 µM and incubated at 37°C for 10 min. Signals were collected by flow cytometry in the fluorescence channel above 600 nm (FL-2 channel). The experiments were repeated at least three times. ***P<0.001 *vs* control cells; $^{§§}P$<0.01 and $^{§§§}P$<0.001 *vs* Fe^{3+} 200 µM-treated cells.

4.4.5. BJe decreases oxidative DNA damage exerted by Fe^{3+}

To investigate the usefulness of the BJe to restrain DNA oxidative damage, we measured the levels of 8-oxo-dG and the DNA strand breaks. The results of cytofluorimetric analysis using FITC-labelled avidin probe are reported in figure 14A. Despite the massive iron-induced DNA damage, the pre-treatment with BJe significantly decreased oxidative DNA damage (P<0.001). In particular, at the higher iron concentration, the levels of 8-oxo-dG were reduced by 70% in the cells treated with 50 µg mL^{-1} of BJe (fig. 14A). This protective effect against iron-induced genotoxicity was confirmed by the Comet-assay (fig. 14B), and TDNA % values were strongly related to 8-oxo-dG values assessed as AFU of FITC-labelled avidin (r= 0.69 P<0.01).

A

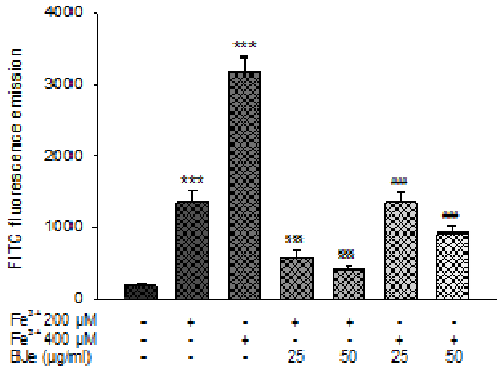

B

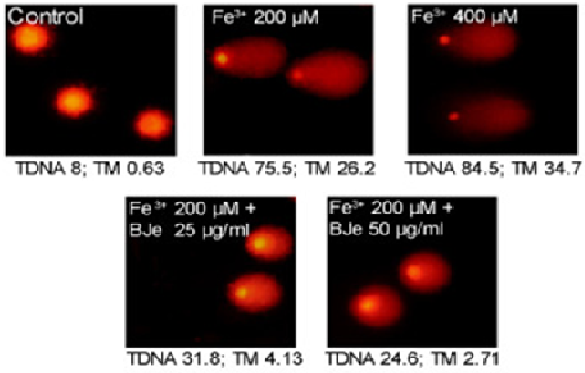

Fig. 14. Effect of BJe on DNA damage induced by Fe^{3+}. (A) Levels of 8-oxo-dG are measured as emission signals of fluorochrome FITC-labelled avidin. The cells permeabilised with methanol (15 min at −20◦C) were incubated with avidin-FITC conjugate (0.2 µM) at 37°C for 1 h, and then the fluorescence was collected in the FL-1 channel. The graph reports the mean of fluorescence of three independent experiments. ***P<0.001 *vs* control cells; $^{§§§}P$<0.001 *vs* Fe^{3+} 200 µM-treated cells; $^{###}$P<0.001 vs Fe^{3+} 400 µM-treated cells. (B) Images of comet assay captured by fluorescence microscopy at a magnification of 400×. A representative experiment that was replicated three times with similar results is shown. Percentages of tail DNA (TDNA) and tail moment (TM) are reported.

4.4.6. Chelating activity of BJe

Although the powerful antioxidant activity of BJe, may be attributable to the activity as radical scavenger, we wanted to assess whether it was also due to its potential iron-chelating activity. By complexing iron, BJe would allow to block upstream the redox activity of the stressor, preventing the downstream cellular ROS overproduction. The

results obtained by using calcein-AM are reported in fig. 15. BJe was able to restore the calcein fluorescence that was decreased of about 2 and 3.5 fold after treatment with $Fe_2(SO_4)_3$ 200 and 400 µM, respectively. Moreover, the chelating effect of BJe at 50 µg mL^{-1} concentration observed in cells treated with iron 200 µM was similar to those recorded using DFPD (P<0.001; fig 15).

Abiotic assay, performed by measuring the decreased emission of rhodamine in Fe^{3+} added to BJe solutions in comparison to the ones in PBS, confirmed the chelating property of the extract. In particular, rhodamine emissions were on average 3 and 2.5 fold lower in the solutions formed by Fe^{3+} (100 µM) and BJe (50 µg mL^{-1}).

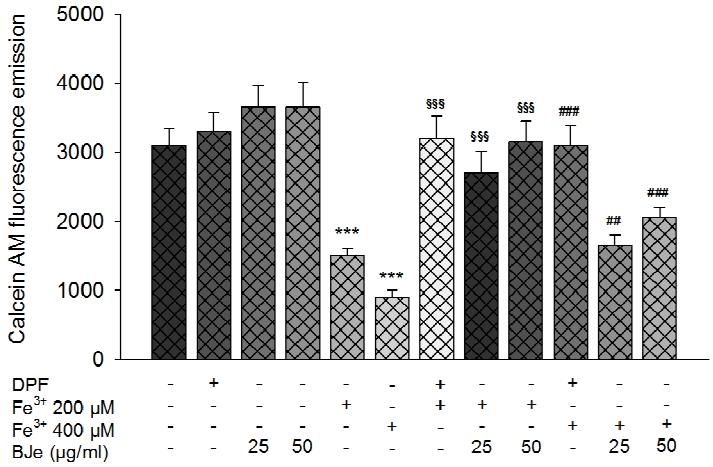

Fig. 15. Evaluation of intracellular free iron. The cells were treated for 18 h with BJe followed by 2 h exposure to Fe^{3+} 200 or 400 µM. The DPF was used as positive control (final concentration: 0.3 M). Calcein-AM probe was used to determine the free iron and fluorescence was acquired by flow cytometry. The experiments were repeated at least three times. ***P<0.001 *vs* control cells; §§§P<0.001 *vs* Fe^{3+} 200 µM-treated cells; ## and ###P<0.01 and P<0.001, respectively *vs* Fe^{3+} 400 µM-treated cells.

4.4.7. Indirect anti-oxidant activity of BJe

To assess the ability of BJe to enhance the expression of defense genes, we assessed the catalase activity. As showed in figure 16 BJe increases the values of both gene

expression and activity of the enzyme in comparison to those observed in basal condition (untreated cells). Moreover, the extract reverts the catalase inhibition caused by iron exposure, doubling the enzyme activity (*P*<0.01).

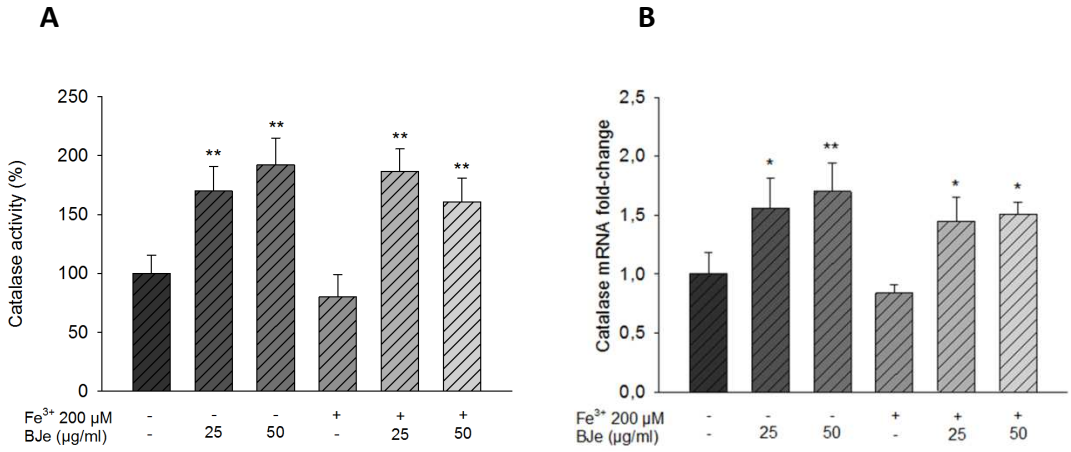

Fig. 16. Effects of BJe on catalase enzyme. The cells were treated for 18 h with BJe followed by 2 h exposure to Fe^{3+}200 µM. (A) Colorimetric evaluation of catalase activity. The obtained results are reported as percentages of catalase activity, detected in untreated cultures. (B) Relative catalase mRNA levels (based on β-Actin). **P*<0.05, ***P*<0.01 *vs* Fe^{3+} 200 µM-treated cells.

4.5. BJe reduces LPS-Induced inflammatory response in THP-1 monocytes

4.5.1. Cell viability assay in presence of LPS

In order to assess BJe toxicity in the THP-1 cell cultures, preliminary experiments were carried out using the MTT test. Exposure of THP-1 monocytes to different BJe concentrations (in a range from 0.05 to 0.5 mg/ml) for 3.5 h did not show any significant reduction of cell viability when BJe was added in presence or absence of LPS (fig. 17).

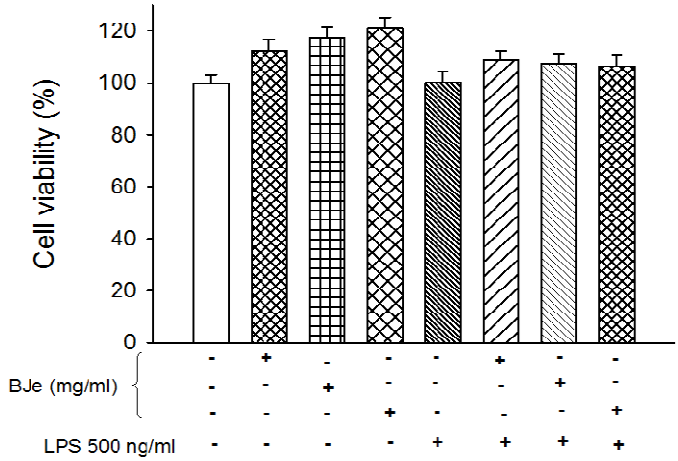

Fig. 17. Effect of BJe on THP-1 cell viability in presence or absence of LPS. Different concentrations of BJe (0.01, 0.05, 0.1 and 0.5 mg/ml) were added to the culture medium 30 min before LPS treatment (500 ng/ml for 3 h) and then cell viability was assessed by the MTT test. Results are expressed as percentages of untreated cultures. Data are means ± S.E.M. of three independent experiments performed in eightplicate.

4.5.2. Expression of LPS-induced pro-inflammatory cytokines in presence of BJe

Based on preliminary experiments, in this study we used LPS at the concentration of 500 ng/ml that was able to trigger the release of pro-inflammatory factors in THP-1 cells within three hours. Under these conditions, the Real-time PCR analysis showed that LPS stimulation of THP-1 monocytes resulted in a dramatic increase of pro-inflammatory cytokines (IL-6, IL-1β, TNF-α) mRNA, relative to endogenous 18S mRNA levels. In particular, IL-6 mRNA increase was higher than those observed for IL-1β and TNF-α. The IL-6 mRNA levels in LPS-treated cells were almost one hundred-fold higher than those found in untreated cells (Fig. 18A). These effects were reduced in presence of BJe. Specifically, LPS-induced IL-6 up-regulation was strongly decreased in presence of BJe 0.05 mg/ml (by ~70%), with a maximum reduction of ~80% with 0.1 mg/ml BJe (P<0.001). Even though to a lesser extent, also BJe 0.5 mg/ml was able to reduce IL-6 mRNA levels (~60%; P<0.001). In parallel, the LPS-induced increase in IL-1β gene expression (36-fold higher than controls) was significantly reduced by all BJe concentrations used (from 70 to 80%; fig. 18B). In a similar way, stimulation of THP-1 monocytes with LPS caused a 5-fold increase of TNF-α mRNA levels in comparison with untreated cells, while a significant downregulation of LPS-stimulated TNF-α gene expression was observed in presence of BJe (in the range 0.05-0.5 mg/ml), resulting in mRNA levels similar to those found in control cells (fig. 18C).

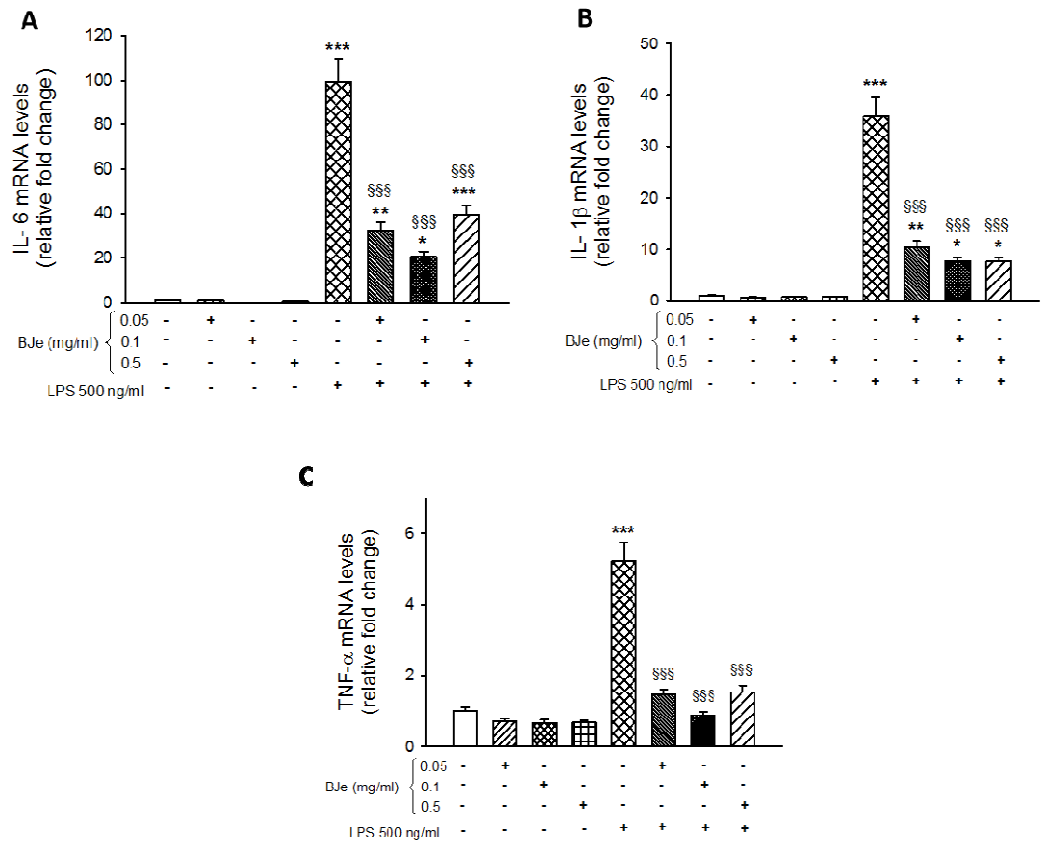

Fig. 18. Effects of BJe on cytokine gene expression in THP-1 cells stimulated with LPS. THP-1 cells were treated with different concentrations of BJe (0.05-0.5 mg/ml for 30 min) before exposure to 500 ng/ml of LPS for 3 h. Results from real-time PCR of IL-6 (A), IL-1β (B) and TNF-α (C) are expressed as a relative fold change compared to untreated cells, after normalization against 18S as endogenous control. Columns and bars represent means ± SEM from triplicate experiments. **P*<0.05, ***P*<0.01, ****P*<0.001 *vs* control cells; §§§*P*<0.001 *vs* LPS-treated cells (ANOVA followed by Student-Newman Keuls multiple comparisons test).

4.5.3. BJe treatment reduces the release of cytokines caused by LPS

In order to confirm the LPS-induced up-regulation of pro-inflammatory genes, we assessed the release of the analyzed cytokines by their detection in the supernatants collected at the end of the treatment. As shown in figure 19, in comparison to untreated cells, 3 h of LPS stimulation was able to trigger the secretion of significant amount of IL-1β and especially of TNF-α (4.7 and 37 fold increases, respectively), but

not of IL-6. These LPS-induced releases were reduced by BJe treatment. In particular, both BJe 0.1 and 0.5 mg/ml significantly decreased the amount of secreted IL-1β by 27 and 25%, respectively (*P*<0.05 *vs* LPS-treated cultures; fig. 19B), while all used BJe concentrations affected the release of TNF-α between 17 and 50% (*P*<0.05 and *P*<0.001 *vs* LPS-treated cells; fig. 19C). Interestingly, the most effective concentration of BJe able to diminish the protein levels of both IL-1β and TNF-α was 0.1 mg/ml.

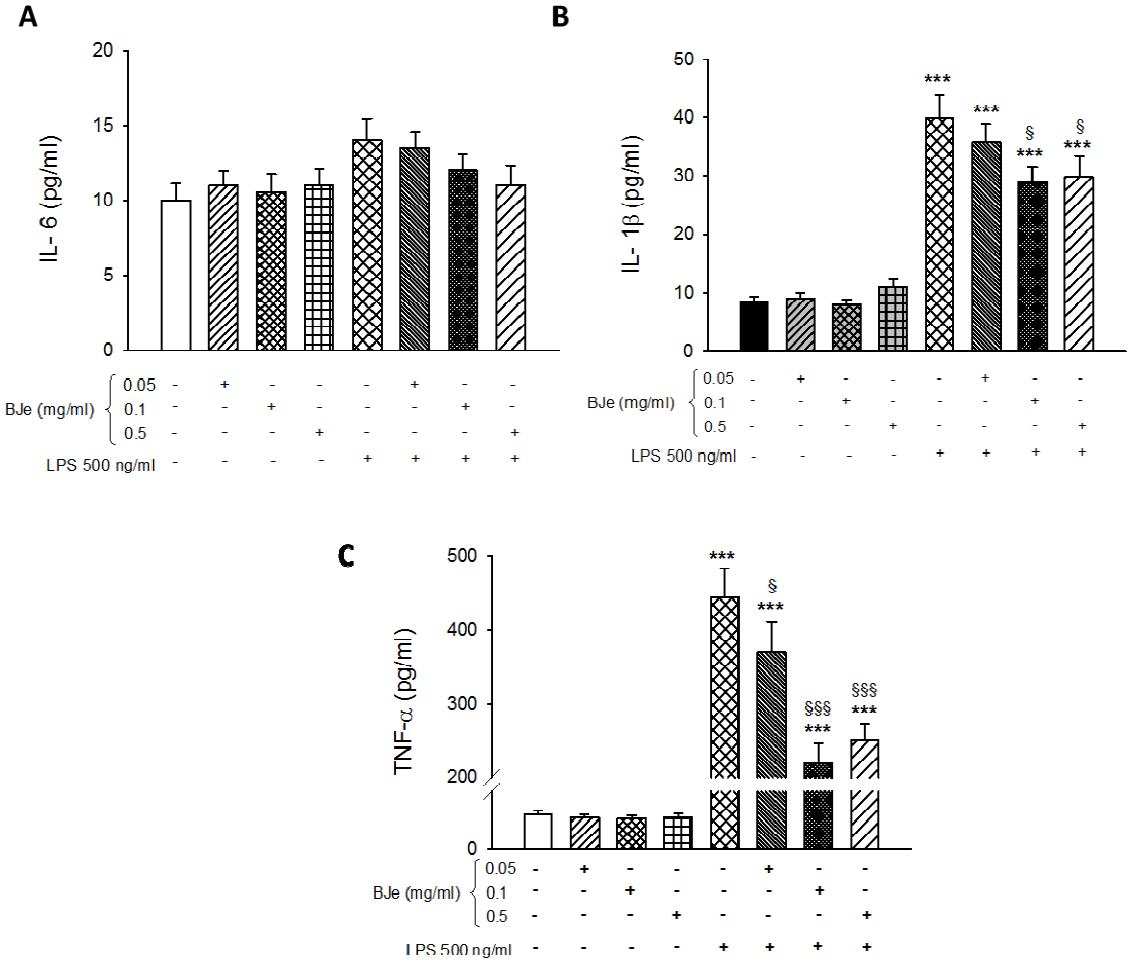

Figure 19. BJe prevents the LPS-stimulated release of IL-1β and TNF-α in THP-1 monocytes. The cells were treated with increasing concentrations of BJe (0.05-0.5 mg/ml for 30 min) prior to add LPS (500 ng/ml; 3 h). Then, secretion of IL-6 (A), IL-1β (B) and TNF-α (C) in the media was evaluated by ELISA assay. Data are the mean ± SEM of three independent experiments performed in triplicate. ***P<0.001 *vs* untreated cultures; $^{§}P$<0.05 and §§§P<0.001 *vs* LPS treated cells (ANOVA followed by Student-Newman Keuls multiple comparisons test).

4.5.4. Inhibition of LPS-induced NF-κB by BJe

Given the reported pivotal role of NF-κB in inflammatory response induced by various stimuli, we also investigated its role in THP-1 cell response to LPS-induced injury, in presence of the most effective concentration of BJe (0.1 mg/ml). EMSA analysis of nuclear fractions showed that nuclear translocation and specific DNA binding activity of NF-κB increased in THP-1 cell cultures, after 3 h of incubation with LPS (fig. 20). Interestingly, BJe 0.1 mg/ml was able to inhibit the LPS-induced NF-κB activation.

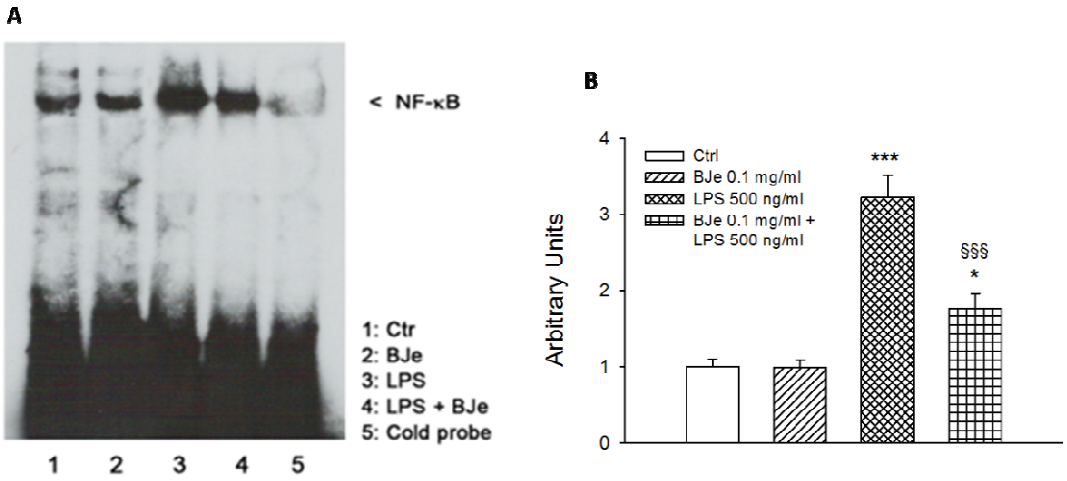

Fig. 20. Inhibitory effect of BJe on LPS-induced NF-κB activation in THP-1 cells. (A) The cells were exposed to 0.1 mg/ml BJe 30 min before LPS treatment (500 ng/ml for 3 h), and then NF-κB activation was determined by the electrophoretic mobility shift assay (EMSA). A competition assay was performed using both biotin-labeled and unlabeled specific probe (cold probe, CP). (B) Densitometric analysis of three independent blots (mean ± S.E.M.) is reported. * and ***P<0.05 and P<0.001 vs untreated cultures, respectively; $^{§§§}P$<0.001 *vs* LPS-treatment (ANOVA followed by student-Newman Keuls multiple comparisons test).

4.5.5. BJe treatment reverts LPS-enhanced acetylation of p65 through the involvement of SIRT1

Since it is known that SIRT1 may suppress inflammation by deacetylation of NF-κB subunit, in a subset of experiments we also investigated its regulatory effects on NF-κB activation. As shown in figure 21, the inhibitory effect of 0.1 mg/ml BJe on the LPS-induced activation of NF-κB was counteracted at highest dose of Sirtinol, the well-known inhibitor of SIRT1. In particular, 10 μM of Sirtinol reverted the NF-κB inhibition due to BJe treatment, suggesting a role of SIRT1 in the modulatory effect of BJe on NF-κB signaling.

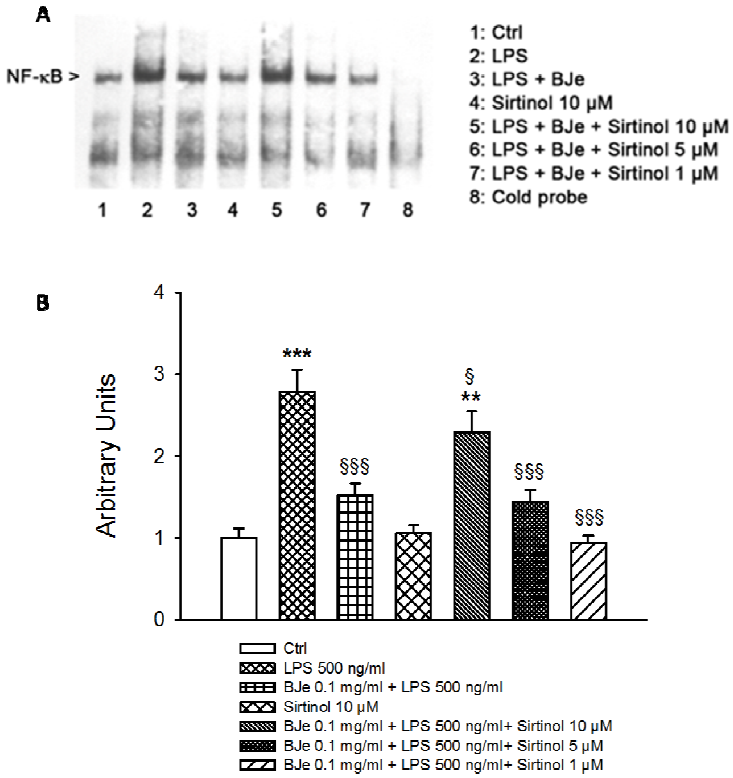

Fig. 21. Sirtinol reverts the inhibitory effect of BJe on LPS-induced activation of NF-κB. (A) Exposure of THP-1cells to 0.1 mg/ml BJe reduced LPS-induced NF-κB activation; this effect was reverted by 10 μM Sirtinol, a SIRT1 inhibitor. EMSA analysis was performed using both biotin labeled and unlabeled specific probe (cold probe). (B) Densitometric analysis of three independent blots (mean ± S.E.M.) is presented. **P<0.01 and ***P<0.001 *vs* controls; $^{§§§}P$<0.001 *vs* LPS-treated cells. $^{\#}$P<0.05 *vs* BJe plus LPS-treated cells (ANOVA followed by Student-Newman Keuls multiple comparisons test).

In order to clarify the involvement of SIRT1 deacetylating activity and the molecular mechanism underlying the BJe mediated inhibition of NF-κB, an immunoprecipitation assay was carried out to evaluate the acetylation status of RelA/p65 subunit. As shown in figure 22, BJe 0.1 mg/ml treatment reverted the LPS-enhanced acetylation of p65 in THP-1 monocytes. In addition, increasing concentrations of Sirtinol were able to suppress the inhibitory effect of BJe on the activation of NF-κB, via p65 acetylation, underscoring that NF-κB–mediated inflammatory cytokines production may be directly linked to SIRT1.

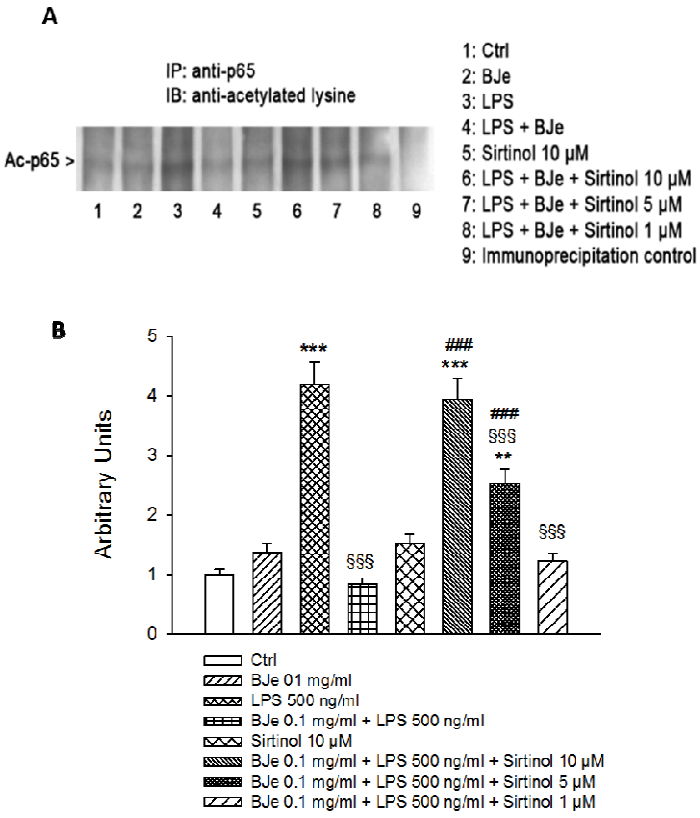

Fig. 22. BJe treatment reverts the LPS-enhanced acetylation of p65 in THP-1 cells. (A) After LPS treatment in presence or absence of BJe and/or Sirtinol, THP-1 cells were lysed and proteins were immunoprecipitated using an anti-p65 antibody. Immunoprecipitated proteins were separated by SDS-PAGE and immunoblotted with antibody against acetyl-lysine residues. Immunoprecipitation negative control was set by incubating cell lysates under similar conditions, but without the immunoprecipitating antibody. (B) Densitometric analysis of three independent blots (mean ± SEM) is presented. ***P*<0.01 and ****P*<0.001 *vs* control cultures; §§§*P*<0.001 *vs* LPS-treated cells; $^{###}$*P*<0.001 vs LPS plus BJe-treated cells (ANOVA followed by Student-Newman Keuls multiple comparisons test).

4.6. BJe attenuates β-amyloid-induced pro-inflammatory activation of THP-1 cells

4.6.1. $A\beta_{1-42}$ causes an increase of pro-inflammatory cytokines gene expression

In order to assess time-dependent effects of fibrillar $A\beta_{1-42}$ on the induction of pro-inflammatory cytokines, THP-1 cells were incubated over a 24 h period in the presence or absence of 0.5 μM $A\beta_{1-42}$. In Aβ-treated cells, there was a rapid increase of TNF-α mRNA transcript level that peaked at 2 h and rapidly declined by 6 h, reaching the basal levels after 16 h of incubation. The mRNA transcript levels of both IL-1β and IL-6 increased in parallel in the presence of $A\beta_{1-42}$ and peaked at 6 h, remaining high until 24 h of incubation (fig. 23A). Cytokine up-regulation was a specific effect of fibrillar $A\beta_{1-42}$, as demonstrated by the parallel treatment with other amyloid peptides that did not induce any significant changes in cytokine mRNA levels (fig. 23B).

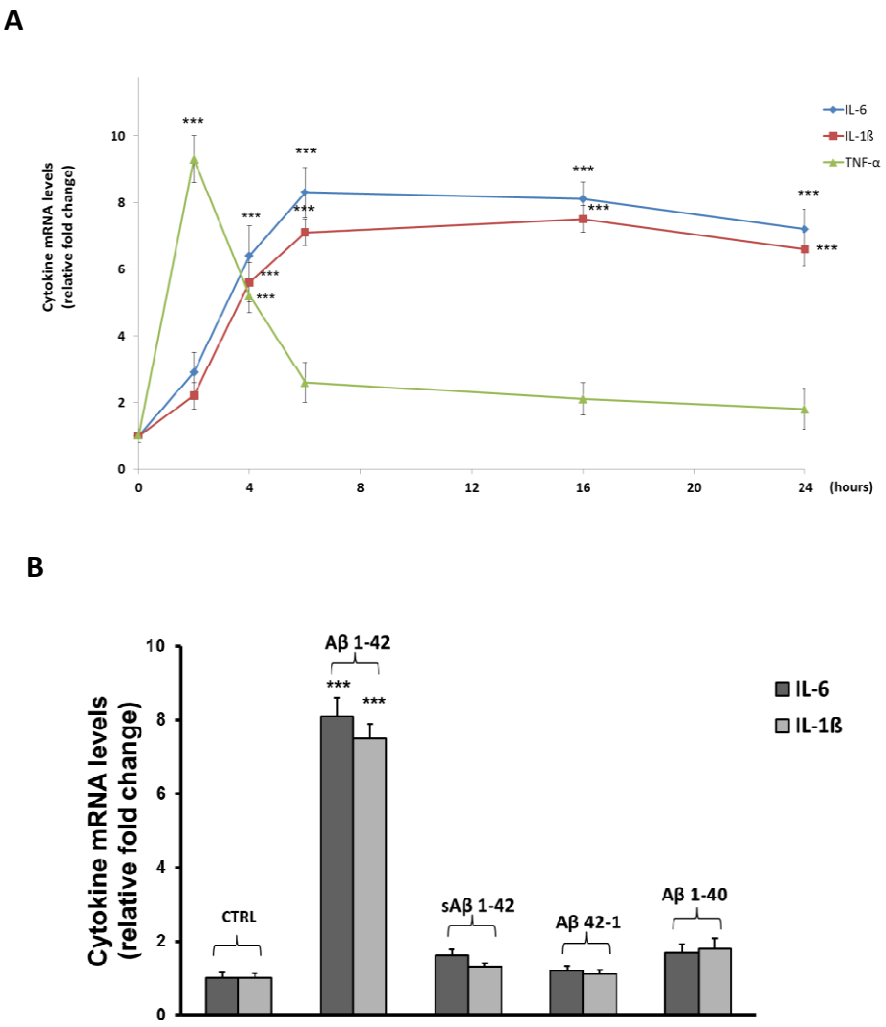

Fig. 23. Cytokine gene expression in THP-1 monocytes exposed to different amyloid peptides. (a) The time course of gene expression for IL-6, IL-1β and TNF-α following incubation with 0.5 μM $A\beta_{1-42}$ in THP-1 cells over a 24 h period is shown. (b) Effects of $A\beta_{1-42}$, $sA\beta_{1-42}$, $A\beta_{42-1}$ and $A\beta_{1-40}$ on cytokine mRNA levels of both IL-6 and IL-1β in THP-1 cells after 16 h of incubation. Results from real-time PCR are expressed as relative fold change of mRNA levels detected in treated cells compared to the untreated culture, after normalization to β-actin as endogenous control. Data represent means ± S.E.M. of three independent experiments. ***P<0.001 *vs* control.

On the basis of these observations a period of 16 h of incubation was chosen as standard incubation time to further test the effects of BJe against $A\beta_{1-42}$-induced pro-inflammatory response.

4.6.2. Effect of $A\beta_{1-42}$ and BJe on THP-1 cell viability and ROS production

Under these conditions, neither significant changes in mitochondrial activity (MTS assay; fig. 24A) nor a reduction of cell membrane integrity (PI exclusion test; fig. 24B) were observed in THP-1 cells when 0.5 μM $A\beta_{1-42}$ was added to cell cultures in presence or absence of different concentrations of BJe. Moreover, the incubation with BJe alone did not affect cell viability (fig. 24A and B).

Treatment with $A\beta_{1-42}$ also induced about two fold increase of intracellular ROS levels (fig. 24C). These effects were blunted by BJe that displayed a more powerful antioxidant effect in comparison with NAC, a well-known ROS scavenger (fig. 24C).

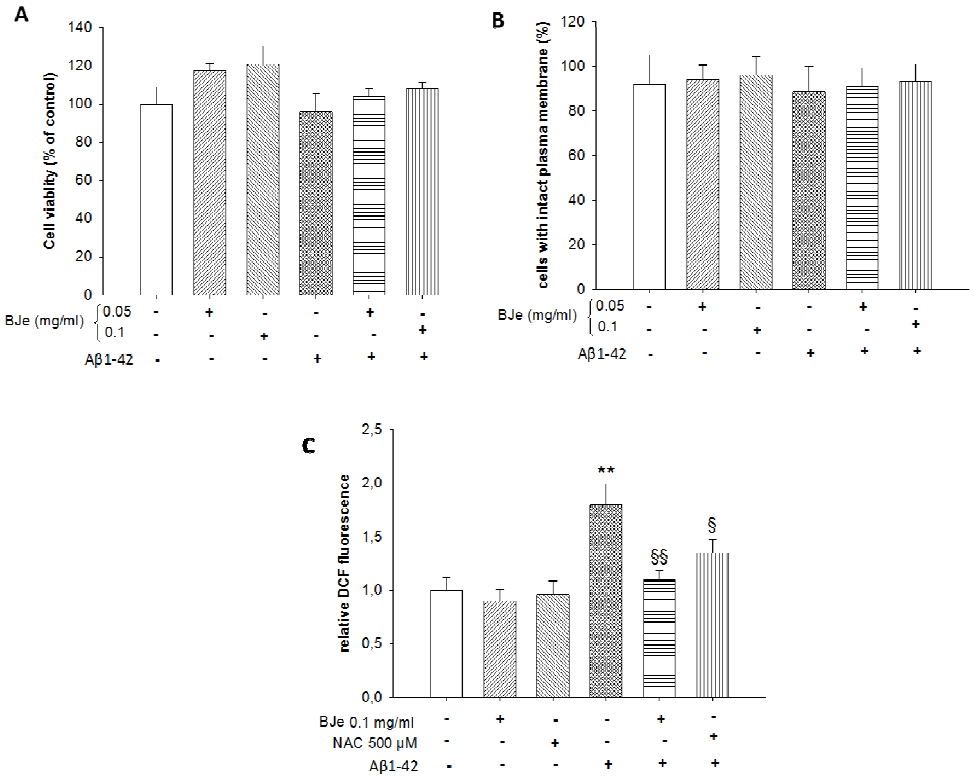

Fig. 24. Effect of $A\beta_{1-42}$ and BJe on THP-1 cell viability and ROS production. Cell viability was assessed by evaluation of mitochondrial activity (A, MTS assay) and membrane integrity (B, propidium iodide assay) in THP-1 cells untreated (Ctrl) or treated for 16 h with 0.5 µM $A\beta_{1-42}$ in the presence or absence of different BJe concentrations, added to the culture medium 3 min prior to $A\beta_{1-42}$ treatment. MTS experiments were performed in octuplicate and repeated three times; the results were expressed as percentage (mean ± S.E.M) of cell viability found in untreated cultures. PI experiments were performed in triplicate and results were expressed as percentage (mean ± S.E.M) of non-fluorescent cells over the total number of cells counted. (C) Evaluation of intracellular ROS levels by fluorimetric measurement of oxidated DCF-DA in cells incubated with/without $A\beta_{1-42}$ in presence or absence of BJe and NAC. $^{**}P<0.01$ *vs* controls. $^{\S}P<0.05$, $^{\S\S}P<0.05$ *vs* $A\beta_{1-42}$-treated THP-1 cells.

4.6.3. BJe reduces IL-1β and IL-6 gene expression and secretion in $A\beta_{1-42}$-treated cells

The pre-incubation with BJe was able to concentration-dependently reduce the $A\beta_{1-42}$-induced increases in both IL-1β and IL-6 mRNA levels; the maximal inhibitory effects were displayed by 0.1 mg/ml BJe (fig. 25A). We also assessed the effects of $A\beta_{1-42}$, in the presence or absence of BJe, on the secretion of both IL-1β and IL-6 after 16 h of incubation, time at which cytokine expression was still maximal. The measurements of

IL-1β and IL-6 amounts released into the medium showed that $A\beta_{1-42}$ increased the release of IL-6 and IL-1β by about 10-fold and 80-fold, respectively, into the medium. These effects were significantly reduced in the presence of BJe, which displayed the maximal effects at a concentration of 0.1 mg/ml reducing IL-6 and IL-1β concentration by about 55% and 39%, respectively (fig. 25B).

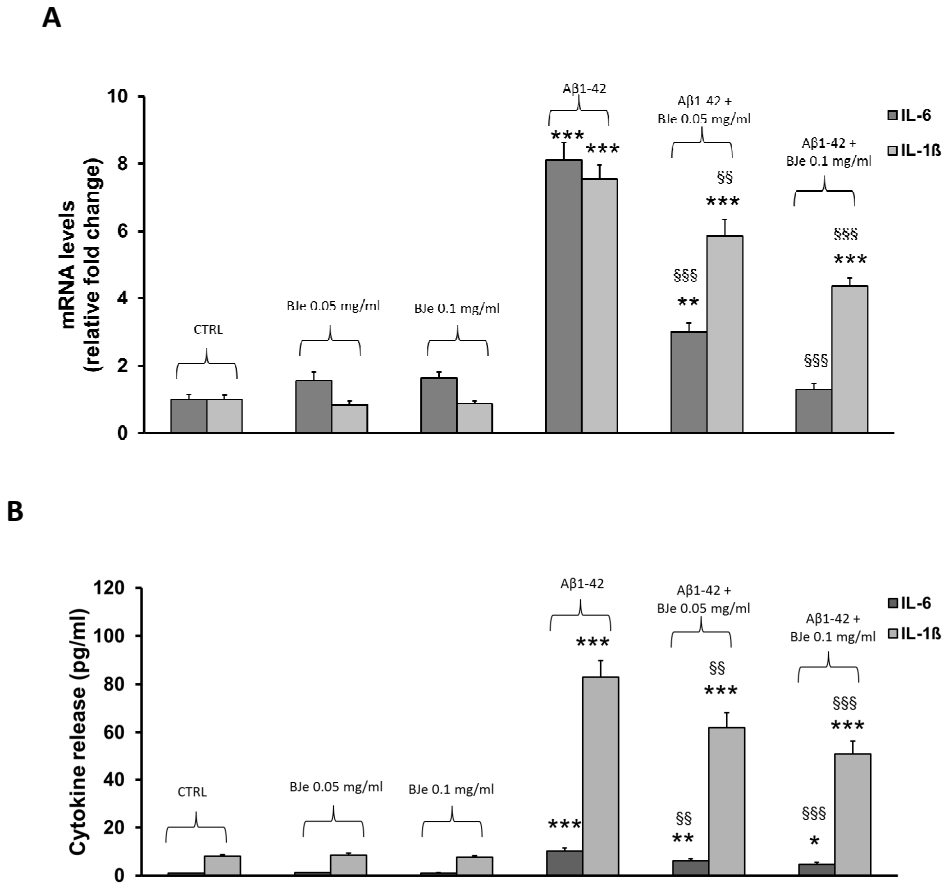

Fig. 25. BJe reduces IL-1β and IL-6 gene expression and secretion in $A\beta_{1-42}$-treated cells. Concentration dependent effects of BJe against $A\beta_{1-42}$-evoked increase in (A) mRNA transcript levels and (B) cytokine release of both IL-6 and IL-1β in THP-1 cells. Quantification of mRNA transcripts was performed by Real-time PCR and expressed as relative fold change in treated cells compared to those found in untreated culture, after normalization to β-actin. Evaluation of secreted cytokines was performed by ELISA in supernatants of THP-1 monocytes treated and untreated with BJe and $A\beta_{1-42}$. Data are provided as pg of cytokines released per ml of culture media. **P*<0.05, ***P*<0.01, ****P*<0.001, statistical differences in comparison to controls. $^{\S\S}P$<0.01, $^{\S\S\S}P$<0.001 *vs* $A\beta_{1-42}$-treated cells. Results from both Real-time PCR and ELISA experiments represent the mean ± S.E.M. of three independent experiments.

4.6.4. BJe decreases the phosphorylation of MAPK caused by $A\beta_{1-42}$

Given that the MAPK super family of enzymes is known to regulate the inflammatory response in many cell lines, we wondered whether the $A\beta_{1-42}$-mediated induction of a pro-inflammatory response in THP-1 cells involved the activation of MAPK members, and whether BJe was able to affect this signaling pathway. After 16 h of incubation with 0.5 µM $A\beta_{1-42}$, we observed a 2.5 fold increase in the amounts of phosphorylated ERK 1/2 as well as p54 JNK, and a fourfold increase in those of phosphorylated p46 JNK, in THP-1 monocytes. No changes were observed in the p38 phosphorylation status under different conditions (fig. 26A and B). The $A\beta_{1-42}$-induced effects were counteracted when THP-1 cells were pre-incubated with BJe. In particular, the levels of phosphorylated p54 and p46 JNK were reduced by 54% and 60%, respectively, and those of phosphorylated ERK 1/2 proteins were reduced by about 45% (fig. 26A and B). Notably, MAPK down-regulation occurred at higher extent in the presence of BJe than NAC. In fact, the reduction of protein levels achieved in the presence of NAC was 44% and 52% for phosphorylated p54 and p46 JNK, as well as 27% and 22% for phosphorylated ERK1 and ERK2, respectively (fig. 26A and B).

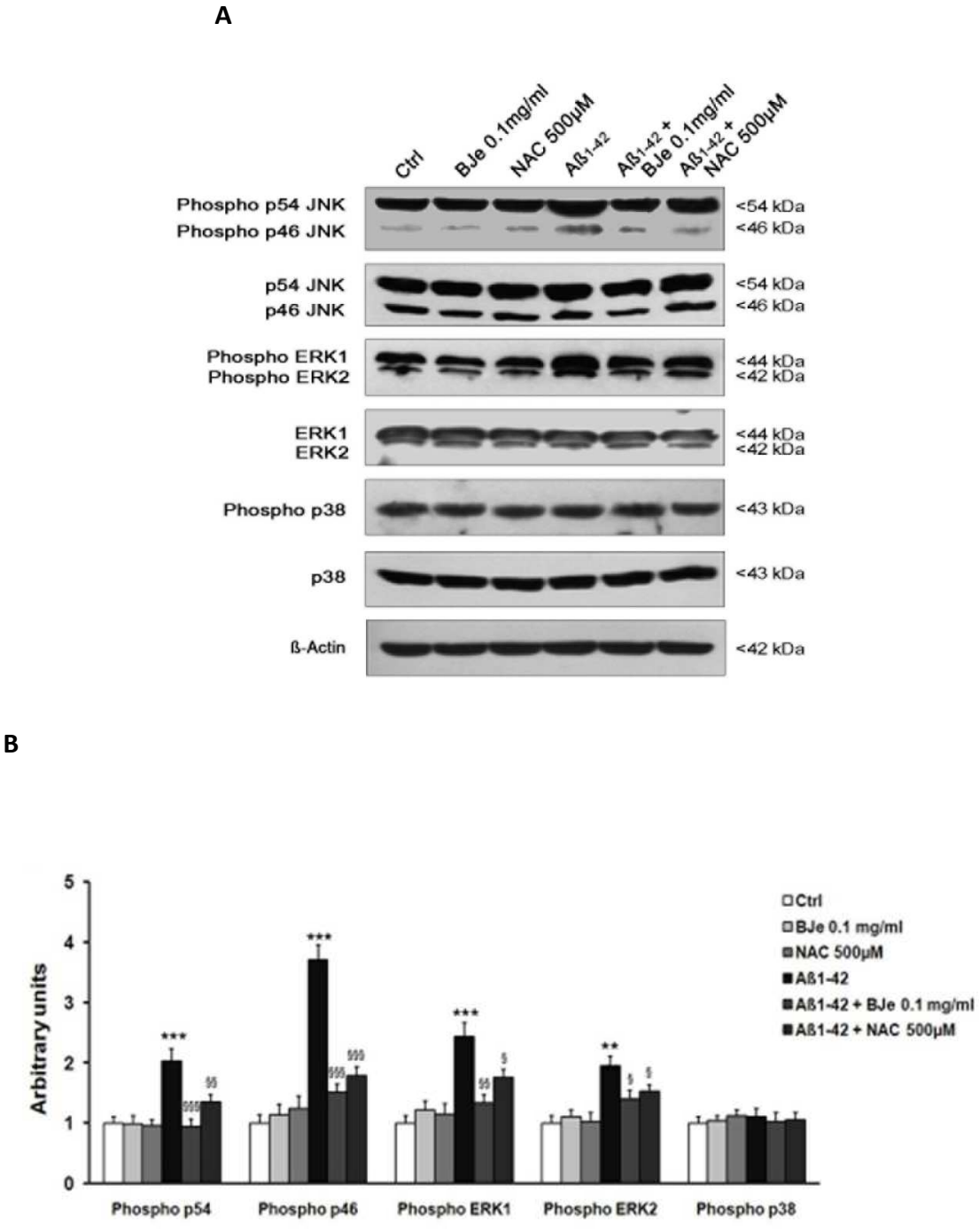

Fig. 26. BJe reduces the phosphorylation of MAPK caused by $A\beta_{1\text{-}42}$. (A) The modulation of MAPK superfamily members by BJe and NAC in THP-1 monocytes exposed to $A\beta_{1-42}$ was evaluated by Western blot analyses, checking the phosphorylated status of MAPK proteins. Representative immunoblot images of p54, p46, p38 and ERK 1/2 are shown. The blot images were cropped around the region of interest and the samples were resolved on gels run under the same experimental conditions. (B) The densitometric analysis of three independent experiments (mean ± S.E.M.) is presented. ***P*<0.01, ****P*<0.001 *vs* controls. $^{\S}P$<0.05, $^{\S\S}P$<0.01, $^{\S\S\S}P$<0.001 *vs* $A\beta_{1-42}$-incubated THP-1 cells.

4.6.5. BJe determines a decrease of AP-1 DNA binding activity in $A\beta_{1-42}$-treated THP-1 cells

We also determined whether the exposure of THP-1 cells to $A\beta_{1-42}$ resulted in the increase of DNA binding activity by transcription factor NF-κB, given the reported involvement of NF-κB activation in cytokine up-regulation in several cell models. However, no significant differences in NF-κB activation levels were observed in THP-1 cells treated with $A\beta_{1-42}$, in the presence or absence of BJe, in comparison with controls (fig. 27A and C). In the light of these results, we wondered whether other transcription factors could be involved in the inflammatory response evoked by $A\beta_{1-42}$ in THP-1 cells. Therefore, given the here observed significant increase of phosphorylated ERK1/2 and p46/p54 JNK levels, we looked at the activation of AP-1, a downstream target of these MAPK members in inflammatory pathways. After 16 h of incubation, we observed a 2.3-fold increase of AP-1 DNA binding activity in nuclear extracts of $A\beta_{1-42}$-treated THP-1 monocytes (fig. 27B and D) compared with control cells. In the presence of BJe (0.1 mg/ml), the $A\beta_{1-42}$-induced increase of AP-1 DNA binding activity was reduced by about 35% (fig. 27B and D).

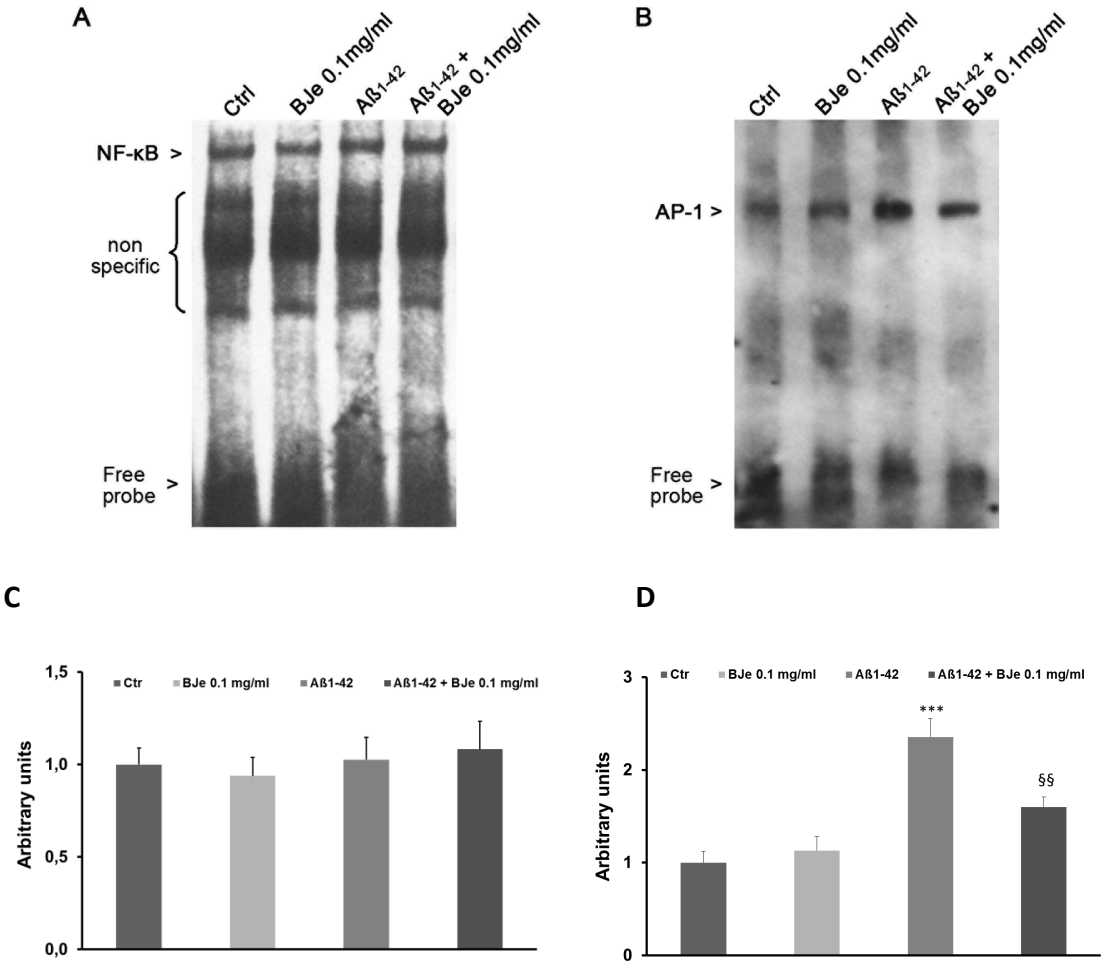

Fig. 27. EMSA analysis of NF-κB and AP-1 in $A\beta_{1-42}$-treated THP-1 cells after exposure to BJe. DNA binding activity of both NF-κB (A) and AP-1 (B) in nuclear extracts of untreated and $A\beta_{1-42}$-treated THP-1 cells in presence or absence of BJe is shown. The densitometric analyses (C and D) of three independent EMSA assay (mean ± S.E.M.) are displayed. ***P<0.001 *vs* controls. §§P<0.01 *vs* $A\beta_{1-42}$-treated cells.

4.6.6. Inhibition of AP-1 DNA binding activity by AP-1 ODN attenuates $A\beta_{1-42}$-nduced up-regulation and secretion of cytokines in THP-1 cells

Finally, to ascertain the role of AP-1 activation in inflammatory response induced by $A\beta_{1-42}$, cell transfection with the AP-1 decoy oligodeoxynucleotide (ODN), an inhibitor of AP-1 activation, was carried out. EMSA analysis showed that treatment with AP-1 ODN significantly attenuated the AP-1 DNA-binding activity in THP-1 cells treated with $A\beta_{1-42}$ (fig.28 A and B). In addition, the AP-1 ODN cell transfection significantly reduced

increase in both gene expression and secretion of IL-1β and IL-6 induced by $A\beta_{1-42}$ (fig. 28C and D).

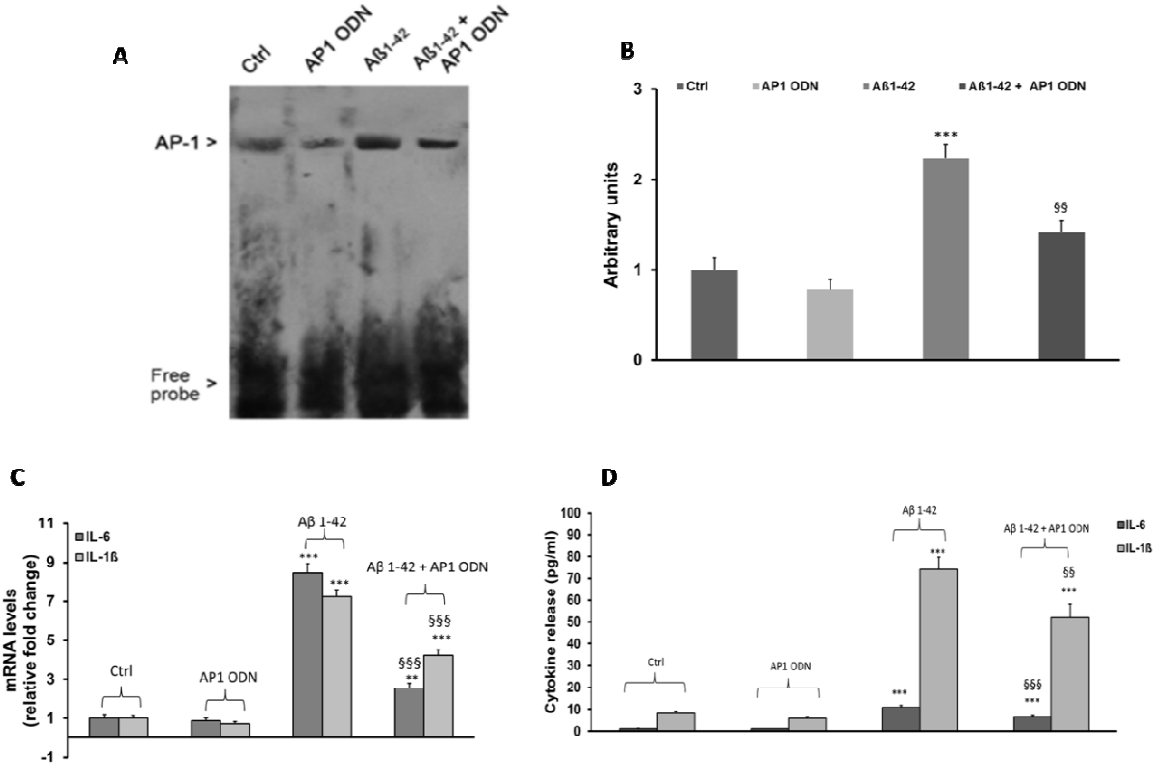

Fig. 28. Inhibition of AP-1 DNA binding activity by AP-1 ODN attenuates $A\beta_{1-42}$-nduced up-regulation and secretion of cytokines in THP-1 cells. The effects of THP-1 cell transfection with AP-1 ODN on AP-1 activation were assessed by EMSA (a) in cells untreated or treated with $A\beta_{1-42}$. Densitometric analysis of three independent blots (mean ± SEM) is reported (b). Evaluation of IL-6 and IL-1β production upon AP-1 ODN mediated AP-1 inhibition was carried out by analysis of cytokine mRNA levels (c) and cytokine release (d) in THP-1 cells untreated and treated with $A\beta_{1-42}$. ***P*<0.01 and ****P*<0.001 *vs* controls. $^{§§}P$<0.01 and $^{§§§}P$<0.001 *vs* $A\beta_{1-42}$-treated THP-1 cells.

5. DISCUSSION

In the last decades, the potential use of natural drugs for prevention and/or adjuvant therapy in chronic degenerative disease linked to oxidative stress, has gained attention of scientific community. Numerous studies were performed to evaluate the anti-oxidant and anti-inflammatory effect of *Citrus* flavonoids used as pure compounds. Moreover, several *in vitro* and *in vivo* research have identified their molecular targets and, consequently, their mechanism of action. These findings highlight the anti-oxidant nature of flavonoids, able to arrest free radical-induced oxidative damage, which is known to play a pivotal role in many inflammatory and degenerative diseases.

In recent years, the beneficial properties of the *C. bergamia* juice have been raising interest and they have been the subject of recent studies due to the broad spectrum of biological properties. Moreover, a very interesting paper (Liu et al., 2004) explains why a single bioactive compound may not replicate the same effect as the phytocomplex in which it is contained. Indeed, often, even at high concentrations, no single active principle can replace the combination of natural phytochemicals present in an extract in achieving the same magnitude of pharmacological effect. Liu (2004) suggests that the additive and synergistic effects of phytochemicals in fruits and vegetables are responsible for this potent anti-oxidant activity, and that the benefits of a diet rich in fruits and vegetables is attributable to the complex mixture of phytochemicals present in whole foods.

On these bases, during my PhD, I focused my studies on the evaluation of the anti-oxidant and anti-inflammatory effects of BJe. The first aim was to chemically characterize the extract which was kindly provided by a *Citrus* company with which we shared a research project. The qualitative and quantitative profile of flavonoids in BJe

was in accordance with typical BJ flavonoid determination reported in the literature (Miceli et al., 2007; Sommella et al., 2013). Since it is known that *Citrus* flavonoids possess antioxidant activity, then we started to investigate this biological property in abiotic experimental models. Results of these studies suggested the potential of our extract, encouraging us to study more in depth the antioxidant ability of our extract. To this aim, we investigated the effects of BJe on H_2O_2-induced oxidative stress in human alveolar type II epithelial A549 cells, which resemble the pathophysiological lung conditions of respiratory epithelium (Hsu et al., 2013). Hydrogen peroxide, commonly used in *in vitro* models as oxidative stress, is a physiological component of living cells and is constantly formed through various cellular pathways. Its intracellular steady state concentration is controlled by several enzymatic and non-enzymatic anti-oxidant systems and is assumed to fluctuate from 1 to 700 nM (Antunes et al., 2001). Although H_2O_2 at physiological concentrations acts as a signaling molecule by modulating the expression of defense genes, levels above 1 μM cause redox imbalance, inducing growth arrest and cell death (Stone and Yang, 2006). Moreover, in the presence of free redox-active transition metals, H_2O_2 contributes to the formation of the hydroxyl radical (·OH), amplifying cellular damage. Due to its high reactivity, ·OH is able to attack DNA, lipids, and proteins, more efficiently than other ROS. H_2O_2 is an important marker of oxidative stress that can be generated by the xanthine/xanthine oxidase reaction, with higher amounts found in *cell-free* bronchoalveolar lavage fluid and plasma taken from patients affected by asthma and other chronic lung disorders, suggesting a central role in their pathogenesis (MacNee et al., 2001). This observation is strengthened by the evidence that patients with lung diseases are characterized by high concentrations of exhaled hydrogen peroxide, which further increases as the

disease exacerbates (MacNee et al., 2001). Moreover, lipid peroxidation byproducts, including 8-isoprostane and hydrocarbons, (e.g., ethane and pentane) are also detectable in the air exhaled by these patients (Paredi et al., 2000; Rahman, 2005), suggesting that membrane lipid peroxidation represents a further key event implicated in lung disorders.

Results of our studies demonstrated that BJe counteract ROS generation induced by H_2O_2 in A549 cells and prevent lipidic hydroperoxides generation, which are precursors of malondialdehyde (MDA) and 4-hydroxynonenal (4-HNE), these being end-products of lipid peroxidation capable of inactivating antioxidant enzymes and causing redox imbalance. In addition, MDA may form adducts with DNA bases, while 4-HNE produces exocyclic etheno-DNA-base adducts (Nair et al., 2007).

The main effect of lipid peroxidation is the dysfunction of mitochondrial membranes causing energy failure and several intracellular events leading to cell death.

It is known that the phospholipids of the internal mitochondrial membrane play a crucial role in optimizing the activity of mitochondrial proteins including several anion carriers, ADP/ATP translocators and some electron transport complexes. Because of the double bonds of their fatty acid constituents, mitochondrial phospholipids are particularly susceptible to peroxidative attack producing organelle impairment. Furthermore, given that modified electron transport complexes causes an additional increase of redox imbalance by endogenous ROS overproduction, a vicious circle is activated, amplifying the oxidative cellular damage (Demedts et al., 2006; Lee et al., 2012). Interestingly, BJe reduced the drop in $\Delta_{\psi m}$ induced by H_2O_2 in A549 cells, thus restoring mitochondrial functions.

In order to thoroughly elucidate the anti-oxidant mechanism of BJe we further investigated its ability to reduce iron-induced oxidative damage in A549 cells. The experimental results evidenced that the anti-oxidant effect of BJe occurs through multiple mechanisms. In particular, BJe induces adaptive response, enhancing cell resistance mechanisms against environmental stress, as shown by the increased catalase activity. In addition to this indirect anti-oxidant effect we revealed its ability to form redox inactive complex with exogenous transition metals.

Our results show that BJe is able to bind Fe^{3+}, thus preventing its reduction that is required to trigger the Fenton reaction and the radical cascade. This reduces intracellular ROS generation and, consequently the oxidative damages of membrane phospholipids and DNA. In fact, the pre-treatment with BJe effectively counteracted the significant ROS overproduction induced by iron. This causes an imbalance of the cellular oxidative homeostasis which in turn determines lipid peroxidation. The strong efficacy of BJe against the significant peroxidative-activity of Fe^{3+} was assessed by the measurements of lipid hydroperoxides that are transient intermediate species from which much more toxic breakdown products are formed, such as 4-HNE and 4-hydroxy-2E-hexenal (4-HHE). These aldehydes, if not neutralized by GSH conjugation, are particularly dangerous, because they form adducts with numerous biomolecules, such as lipoproteins, phosphatidylethanolamine and nucleotides.

Mitochondrial lipid peroxidation can cause impairment of this organelle, due to the very high content of polyunsaturated fatty acids present in their membrane. Mitochondria dysfunction determines energetic failure, amplifying oxidative stress (Di Pietro et al., 2011). Interestingly, BJe, sequestering iron, reduces Fe^{3+}-induced drop of $\Delta_{\psi m}$ in A549 cells, thus improving the mitochondrial functions.

Transition metals are also implicated in oxidative DNA damage (Knaapen et al., 2002), whom hallmarks is the content of 8-OH-dG and DNA strand breaks. Using both these genotoxic biomarkers, we observed that the consistent increases of DNA oxidative damage Fe^{3+}-induced were significantly countered by BJe.

It has been reported that an excessive production of ROS/RNS can initiate the inflammatory machinery that may determine synthesis and secretion of pro-inflammatory cytokines. Accumulating evidences suggest that chronic inflammation represents the main contributing factor to several chronic degenerative pathologies. Several findings have shown that polyphenols exert anti-inflammatory activity in both *in vitro* and *in vivo* models, by modulation of pro-inflammatory gene expression such as COX-2, iNOS and several pivotal cytokines (Middleton et al., 2000; González et al., 2001). Because of their properties, flavonoids might be reasonable candidates for the development of new anti-inflammatory drugs, even if their mechanism of action remains not fully understood.

Numerous results demonstrate that THP-1 monocyte/macrophages are a sensitive *in vitro* model to evaluate potential anti-inflammatory activity of different substances, so that it may be an accurate model to study LPS-dependent inflammatory response (Sharif et al., 2007; Sakharwade et al., 2013; Kim and Kim, 2014). Therefore, we examined the modulating effects of BJe on the LPS-stimulated THP-1 cells.

According to the results obtained by other researchers (Chanput et al., 2010; Schildberger et al., 2013), the gene expression of pro-inflammatory cytokines such as IL-1β, TNF-α and IL-6 increased within the first hours of the LPS challenge, while changes in the secretion pattern of related cytokines did not show similar extent. However, between amount of cytokines secreted from THP-1 monocytes and mRNA

levels of corresponding genes can be also explained by differences in RNA stability, post-translational modification factors and proteolytic processing events that make the production of individual cytokines different (Hegde et al., 2004). Under our experimental conditions, the secreted amount of both TNF-α and IL-1β, but not that of IL-6, were higher than controls, suggesting a general relation between mRNA and protein levels in LPS-stimulated monocyte/macrophages. We demonstrated that BJe is able to significantly reduced both transcription profile and protein levels of pro-inflammatory cytokines. Moreover, we reported a concentration-dependent effect of BJe in a range useful to exclude toxic effects in THP-1 cultures.

The induction of most genes involved in the inflammatory response was eliminated or attenuated under the inactivation of IKK/NF-κB pathway. Since NF-κB plays a pivotal role in coordinating cellular response to infections, stress and injury, it has become a target for numerous anti-inflammatory drugs. Moreover, during the last years several studies have focused on polyphenols, which would act as activators of SIRT1, a member of the class III HDAC family that has been involved in modulating epigenetic gene silencing and cell survival, via acetylation of several both histonic and non-histonic substrates. Recent studies suggest that SIRT1 inhibited the NF-κB signaling through deacetylation of p65/RelA. Therefore, the activation of SIRT1 could alleviate a multitude of NF-κB-driven inflammatory and metabolic disorders (Yao and Rahman, 2012; Xie et al., 2013). On these bases, we investigated the modulatory effect of BJe on a LPS-induced inflammatory response, focusing on SIRT1-mediated NF-κB inhibition. Our results provide evidence for BJe impact on NF-κB pathway, likely via SIRT1 activation. In order to confirm our hypothesis we tested the effects of Sirtinol, a synthetic molecule that inhibits SIRT1 functionality by occupying the site which

normally functions as the binding site for the adenine base of NAD^+ (Trapp et al., 2006). Under our experimental conditions, we observed that Sirtinol triggered RelA/p65 binding in the nuclear fraction of LPS-activated cells. Finally, immunoprecipitation assay suggested that Sirtinol and BJe produced opposite effects on SIRT1 deacetylating activity. Considering the Sirtinol-mediated inhibition of SIRT1 and that BJe could act as SIRT1 activators, these results underline at molecular levels that the BJe-mediated inhibition of NF-κB may be linked to acetylation status of p65/RelA subunit.

It is well-known that the mechanisms responsible for the transduction and amplification of inflammatory responses contribute to the development of neurotoxicity. Hallmarks of chronic inflamed tissues are the presence of an increased number of monocytes, as well as monocyte-derived tissue macrophages that can be referred to microglial cells in the central nervous system (McGeer and McGeer, 2010). Chronic immune activation, caused by different stimuli, can be considered a common feature of chronic neurodegenerative disorders, including Alzheimer's disease (AD) and Parkinson's disease (PD). AD is characterized by the presence of reactive microglia around senile plaques, abundant intracellular neurofibrillary tangles, and progressive loss of neurons in the brains of affected patients (Selkoe, 2001). The plaques are primarily composed of Aβ peptide fibrils assembled by non-covalent polymerization of Aβ monomers that derive from the enzymatic cleavage of amyloid precursor protein (APP; Selkoe, 2004). Noteworthy, Aβ peptides drive cerebral neuro-inflammation by activating microglia and astrocytes, which in turn promote the expression of inflammatory cytokines, the activation of the complement cascade, and the induction of inflammatory enzyme systems (Cameron and Landreth, 2010). The accumulation of

Aβ is thought to be an early and perhaps necessary feature of AD (Selkoe, 2001). The predominant forms of Aβ are the (1–40) and (1–42) fragments. In AD, the presence of monocytes/macrophages in the blood vessel walls and activated microglial cells in the brain parenchyma has been associated with increased deposition of Aβ within the brain (Saresella et al., 2014). However, there is evidence that Aβ deposition initiates a microglia-mediated inflammatory response that culminates in neuronal loss and cognitive decline in AD (Akiyama et al., 2000).

Given that flavonoids were shown to display protective effects against both pro-oxidant and inflammatory stimuli, the last step of the research performed during my PhD was aimed to evaluated the ability of BJe to modulate $A\beta_{1-42}$-mediated pro-inflammatory activation of THP-1 monocytes.

The inflammatory response to Aβ has been studied in numerous *in vitro* models including both microglial and monocytic cells (Klegeris et al., 1997; Yates et al., 2000; Yamada et al., 2009; Zhang et al., 2013). Aβ deposition in the brain triggers a microglia-mediated inflammatory response that contributes to neuronal apoptosis and loss of memory that are characteristic of AD (Heneka et al., 2010). Indeed, the oligomeric aggregates of $A\beta_{1-42}$ are structurally similar in size and appearance to the Aβ-derived diffusible ligands (ADDLs), which have been detected in the cerebrospinal fluid (CSF) of Alzheimer's disease subjects (Georganopoulou et al., 2005). Therefore, in order to elucidate the $A\beta_{1-42}$ effects on the activation of monocytes/macrophages, we exposed the human THP-1 monocytes to $A\beta_{1-42}$ aggregates. Notably, THP-1 monocytes have already been shown to be activated by fibrillar $A\beta_{1-42}$ as well as the non-physiological peptide fragment $A\beta_{1-40}$, with the result of an increase in the production of different pro-inflammatory cytokines (Giri et al., 2003). Furthermore, other observations

suggest that early oligomeric $A\beta_{1-42}$ aggregates may have a role in transforming monocytes *in vivo* (Crouse et al., 2009). These findings are relevant since it has been shown that peripheral hemopoietic cells (e.g., monocytes) are able to cross the blood brain barrier (BBB) and differentiate into microglial cells in the brain parenchyma, suggesting that microglial cells arise from peripheral hemopoietic cells (Hickey et al., 1988; Eglitis et al., 1997). Indeed, the co-localization of Aβ peptide with activated microglial cells in AD brains was confirmed by histological studies (Uchihara et al., 1997).

The treatment with fibrillar $A\beta_{1-42}$ induced up-regulation and secretion of IL-6 and IL-1β in THP-1 monocytes, two molecular events that were reduced in a concentration-dependent way by the pre-incubation with BJe. Given that monocytes/macrophages play a critical role in the inflammatory processes associated with neurodegeneration, this experimental model may represent a useful approach to evaluate the molecular mechanisms underlying the beneficial effects of BJe against neuro-inflammation.

Several studies have shown that the anti-inflammatory properties of *Citrus* flavonoids are due to the inhibition of both synthesis and biological activities of different pro-inflammatory mediators, mainly the arachidonic acid derivatives, prostaglandins E2, F2 and thromboxane A2. In addition, there are well-known anti-oxidant and anti-inflammatory properties of *Citrus* flavonoids that can play an important role against several degenerative pathologies including brain diseases (Benavente-Garcia and Castillo, 2008). In this regard, we observed that BJe displayed a stronger anti-oxidant effect than NAC, the well-known ROS scavenger, against $A\beta_{1-42}$-induced increase of ROS levels.

According with observations by Giri and co-workers (Giri et al., 2003), our results indicate that the up-regulation of IL-6 and IL-1β induced by fibrillar $A\beta_{1-42}$ in THP-1 monocytes is not dependent by NF-κB activation. In this regard, it is noteworthy that both $A\beta_{1-40}$ and $A\beta_{25-35}$, at higher concentrations than those used in this study, have been shown to cause NF-κB activation in THP-1 monocytes (Combs et al., 2001). On the basis of present results, it is likely that $A\beta_{1-42}$ is able to trigger a pro-inflammatory response in THP-1 monocytes through the activation of receptor-mediated signaling, involving kinases such as ERK and JNK, but not p38, as previously reported by Giri and co-workers (Giri et al., 2003). We also observed that the levels of phosphorylated ERK1/2 and JNK in THP-1 incubated with $A\beta_{1-42}$ plus BJe were significantly lower in comparison to those found in THP-1 incubated with $A\beta_{1-42}$ alone.

Plant polyphenols in general and flavonoids in particular have long been considered effective MAPK inhibitors. Indeed, it has been shown that flavonoids limited inflammatory responses to numerous agents by inhibition of ERK phosphorylation (Santangelo et al., 2007, Sarkar et al., 2009). In this study, the pre-incubation with BJe did not significantly affect the basal levels of phosphorylated MAPK proteins, but significantly inhibited $A\beta_{1-42}$-induced MAPK activation through the reduction of phosphorylated ERK1/2 as well as JNK levels. Notably, it has been recently shown that BJe may inhibits MAPK phosphorylation in human colon carcinoma HT-29 (Visalli et al., 2014). Moreover, it has been reported that various flavonoids are responsible for the specific inhibition of different kinases, since they have close structural homology to the PD98059, a MAPK inhibitor (Spencer, 2007). Inhibition of MAPK could be the result of BJe antioxidant activity, acting as a free radical scavenger in a way that is similar to how NAC works. Alternatively, it is possible that the flavonoids of BJe exert an anti-

inflammatory action due to their ability to affect the activation of MAPK pathway promoted by the interaction between $A\beta_{1-42}$ and the receptor for advanced glycation end product (RAGE). More likely, the anti-inflammatory and anti-oxidant activity of BJe is due to its ability to both destroy free radicals and interplay with specific intracellular targets involved in the neurotoxicity of $A\beta_{1-42}$. These findings strengthen our observation on the potential of BJe as nutraceuticals or functional food and supplements in the context of a multi-target pharmacological strategy in the inflammation field.

Previous studies showed that molecules present in BJe inhibit kinases, thus increasing the antioxidant cellular defenses mainly via the ERK/Nrf2 signaling pathway (Parhiz et al., 2015). It has been reported that hesperetin modulates MAP kinase signaling by both increasing (Pollard et al., 2006; Li et al., 2011) or inhibiting (Yoshida et al., 2010) the phosphorylation of ERK1/2, depending by the experimental model. Also naringin is able to either inhibit (Nie et al., 2012, Chen et al., 2014) or activate (Kim et al., 2008; Lee et al., 2008) ERK1/2 and JNK, dependently on the cell line and the experimental model used. However, a peculiarity of our study was that we used a natural extract, in which the 20 flavonoids identified can induce pharmacological effects through a network of synergies and antagonisms that together contribute to determine the biological effect of the phytocomplex.

Although NF-κB is commonly involved in the transcriptional up-regulation of inflammatory mediators, some results show that increases in cytokine expression may be also due to different transcription factors, such as AP-1 (Vukic et al., 2009; Roman et al., 2000). Indeed, many inflammation-related genes not only contain κB sites but also AP-1 binding sites in their promoters. Here we demonstrated that AP-1 DNA

binding activity is involved in the $A\beta_{1-42}$-induced pro-inflammatory activation of THP-1 monocytes. Notably, the incubation with BJe blocked the DNA-binding activity of AP-1, and this effect was likely associated with the significant reduction of phosphorylated JNK and ERK1/2 levels. Moreover, AP-1inhibition by AP-1 ODN was associated with a significant reduction of cytokine production in THP-1 cells exposed to $A\beta_{1-42}$. These hallmark features collectively provide evidence for the involvement of AP-1/JNK signaling pathway in THP-1 cells stimulated by $A\beta_{1-42}$. Therefore, the modulation of these molecular events by BJe well explains its protective effect against $A\beta_{1-42}$-induced increases in cytokine expression and release.

Considering that monocytes play a relevant role in neurodegenerative diseases, through their activation and migration across the BBB and their ability to initiate the inflammatory process, these data provide evidence that the BJe could be effective to reduce the inflammatory response caused by fibrillar amyloid peptides in monocytes/microglial cells.

6. CONCLUDING REMARKS

Numerous *in vitro* and *in vivo* studies have shown the ability of flavonoids to exert anti-inflammatory effects, acting not only as free radical scavengers but also as modulators of several key molecular events implicated in the inflammatory processes. The anti-inflammatory properties of some BJ flavonoids as pure compounds have been extensively investigated and well established in several experimental models (Benavente-Garcia and Castillo, 2008; Manthey et al., 2001; Parhiz et al., 2015), while few studies have focused on the pharmacological activity of *Citrus* juices and extracts and its molecular mechanisms.

To our best knowledge, we were the first to study the anti-inflammatory activity of the flavonoid-rich extract of bergamot juice, suggesting that given the multi-factorial pathogenesis of inflammation, the complex mixture of phytochemicals present in a whole extract acts better than a single constituent. This is because all molecules present in a phytocomplex can simultaneously modulate different targets of action in both human cells and microorganisms, leading to a pool of pharmacological effects contributing together to improve patient's health.

6. BIBLIOGRAPHY

Akiyama H, Barger S, Barnum S, Bradt B, Bauer J, Cole GM, Cooper NR, Eikelenboom P, Emmerling M, Fiebich BL, Finch CE, Frautschy S, Griffin WS, Hampel H, Hull M, Landreth G, Lue L, Mrak R, Mackenzie IR, McGeer PL, O'Banion MK, Pachter J, Pasinetti G, Plata-Salaman C, Rogers J, Rydel R, Shen Y, Streit W, Strohmeyer R, Tooyoma I, Van Muiswinkel FL, Veerhuis R, Walker D, Webster S, Wegrzyniak B, Wenk G, Wyss-Coray T (2000). Inflammation and Alzheimer's disease. Neurobiol Aging 21(3):383-421.

Ambade A, Mandrekar P (2012). Oxidative stress and inflammation: essential partners in alcoholic liver disease. Int J Hepatol 2012:853175. doi: 10.1155/2012/853175.

Antunes F, Cadenas E (2001). Cellular titration of apoptosis with steady state concentrations of H(2)O(2): submicromolar levels of H(2)O(2) induce apoptosis through Fenton chemistry independent of the cellular thiol state. Free Radic Biol Med 30(9):1008-18. doi: 10.1016/S0891-5849(01)00493-2.

Beckman KB, Ames BN (1998). The free radical theory of aging matures. Physiol Rev 78(2):547-81.

Benavente-García O and Castillo J (2008). Update on uses and properties of C*itrus* flavonoids: new findings in anticancer, cardiovascular, and anti-inflammatory activity. J Agric Food Chem 56(15):6185-205. doi: 10.1021/jf8006568.

Bierhaus A, Humpert PM, Morcos M, Wendt T, Chavakis T, Arnold B, Stern DM, Nawroth PP (2005). Understanding RAGE, the receptor for advanced glycation end products. J Mol Med (Berl) 83(11):876-86. doi: 10.1007/s00109-005-0688-7.

Biswas SK, de Faria JB (2007). Which comes first: renal inflammation or oxidative stress in spontaneously hypertensive rats? Free Radic Res 41(2):216-24. doi: 10.1080/10715760601059672.

Biswas SK, Peixoto EB, Souza DS, de Faria JB (2008). Hypertension increases pro-oxidant generation and decreases antioxidant defense in the kidney in early diabetes. Am J Nephrol 28(1):133-42. doi: 10.1159/000109993.

Cabantchik ZI (2014). Labile iron in cells and body fluids: physiology, pathology, and pharmacology. Front Pharmacol 5:45. doi: 10.3389/fphar.2014.00045.

Cachofeiro V, Goicochea M, de Vinuesa SG, Oubiña P, Lahera V, Luño J (2008). Oxidative stress and inflammation, a link between chronic kidney disease and cardiovascular disease. Kidney Int Suppl. (111):S4-9. doi: 10.1038/ki.2008.516.

Cameron B, Landreth GE (2010). Inflammation, microglia, and Alzheimer's disease. Neurobiol Dis 37(3):503-9. doi: 10.1016/j.nbd.2009.10.006.

Caramori G, Adcock IM, Casolari P, Ito K, Jazrawi E, Tsaprouni L, Villetti G, Civelli M, Carnini C, Chung KF, Barnes PJ, Papi A (2011). Unbalanced oxidant-induced DNA damage and repair in COPD: a link towards lung cancer. Thorax 66(6):521-7. doi: 10.1136/thx.2010.156448.

Chanput W, Mes J, Vreeburg RA, Savelkoul HF, Wichers HJ (2010). Transcription profiles of LPS-stimulated THP-1 monocytes and macrophages: a tool to study inflammation modulating effects of food-derived compounds. Food Funct 1(3): 254–61. doi: 10.1039/c0fo00113a.

Chen J, Guo R, Yan H, Tian L, You Q, Li S, Huang R, Wu K (2014). Naringin inhibits ROS-activated MAPK pathway in high glucose-induced injuries in H9c2 cardiac cells. Basic Clin Pharmacol Toxicol 114(4):293-304. doi: 10.1111/bcpt.12153.

Chen C, Kong AN (2005). Dietary cancer-chemopreventive compounds: from signaling and gene expression to pharmacological effects. Trends Pharmacol Sci 26(6):318-26. doi: 10.1016/j.tips.2005.04.004.

Cirmi S, Bisignano C, Mandalari G, Navarra M (2016a). Anti-infective potential of *Citrus bergamia* Risso et Poiteau (bergamot) derivatives: a systematic review. Phytother Res 30(9):1404-11. doi: 10.1002/ptr.5646.

Cirmi S, Ferlazzo N, Lombardo GE, Maugeri A, Calapai G, Gangemi S, Navarra M (2016b). Chemopreventive Agents and Inhibitors of Cancer Hallmarks: May *Citrus* Offer New Perspectives? Nutrients 8(11) E698. doi: 10.3390/nu8110698.

Cirmi S, Ferlazzo N, Lombardo GE, Ventura-Spagnolo E, Gangemi S, Calapai G, Navarra M (2016c). Neurodegenerative Diseases: Might *Citrus* Flavonoids Play a Protective Role? Molecules 21(10) E1312. doi: 10.3390/molecules21101312.

Combs CK, Karlo JC, Kao SC, Landreth GE (2001). beta-Amyloid stimulation of microglia and monocytes results in TNFalpha-dependent expression of inducible nitric oxide synthase and neuronal apoptosis. J Neurosci 21(4):1179-88.

Corasaniti MT, Maiuolo J, Maida S, Fratto V, Navarra M, Russo R, Amantea D, Morrone LA, Bagetta G (2007). Cell signaling pathways in the mechanisms of neuroprotection afforded by bergamot essential oil against NMDA-induced cell death *in vitro*. Br J Pharmacol 151(4):518-29. 10.1038/sj.bjp.0707237.

Cotran R, Kumar V, Collins T (1999). Acute and chronic inflammation. In Robbins and Cotran Pathologic Basis of Disease, 7th ed.; Saunders: Philadelphia, PA, USA 47–87.

Crouse NR, Ajit D, Udan ML, Nichols MR (2009). Oligomeric amyloid-beta(1-42) induces THP-1 human monocyte adhesion and maturation. Brain Res 1254:109-19. doi: 10.1016/j.brainres.2008.11.093.

Dávalos A, Gómez-Cordovés C, Bartolomé B (2004). Extending applicability of the oxygen radical absorbance capacity (ORAC-fluorescein) assay. J Agric Food Chem 52(1):48-54. doi: 10.1021/jf0305231.

Delle Monache S, Sanità P, Trapasso E, Ursino MR, Dugo P, Russo M, Ferlazzo N, Calapai G, Angelucci A, Navarra M (2013). Mechanisms underlying the anti-tumoral effects of *Citrus bergamia* juice. PLoS One 8(4):e61484. doi: 10.1371/journal.pone.0061484.

Demedts IK, Demoor T, Bracke KR, Joos GF, Brusselle GG (2006). Role of apoptosis in the pathogenesis of COPD and pulmonary emphysema. Respir Res 7:53. doi: 10.1186/1465-9921-7-53.

Dias DA, Urban S, Roessner U (2012). A historical overview of natural products in drug discovery. Metabolites 2(2):303-36. doi: 10.3390/metabo2020303.

Di Matteo V, Esposito E (2003). Biochemical and therapeutic effects of antioxidants in the treatment of Alzheimer's disease, Parkinson's disease, and amyotrophic lateral sclerosis. Curr Drug Targets CNS Neurol Disord 2(2):95-107.

Di Pietro A, Baluce B, Visalli G, La Maestra S, Micale R, Izzotti A (2011). *Ex vivo* study for the assessment of behavioral factor and gene polymorphisms in individual susceptibility to oxidative DNA damage metals-induced. Int J Hyg Environ Health 214(3):210-8. doi: 10.1016/j.ijheh.2011.01.006.

Di Pietro A, Visalli G, Munaò F, Baluce B, La Maestra S, Primerano P, Corigliano F, De Flora S (2009). Oxidative damage in human epithelial alveolar cells exposed *in vitro* to oil fly ash transition metals. Int J Hyg Environ Health 212(2):196-208. doi: 10.1016/j.ijheh.2008.05.005.

Duracková Z (2010). Some current insights into oxidative stress. Physiol Res 59(4):459-69.

Eglitis MA, Mezey E (1997). Hematopoietic cells differentiate into both microglia and macroglia in the brains of adult mice. Proc Natl Acad Sci U S A 94(8):4080-5.

Esposito BP, Breuer W, Sirankapracha P, Pootrakul P, Hershko C, Cabantchik ZI (2003). Labile plasma iron in iron overload: redox activity and susceptibility to chelation. Blood 102(7):2670-7. doi: 10.1182/blood-2003-03-0807.

Ferlazzo N, Cirmi S, Calapai G, Ventura-Spagnolo E, Gangemi S, Navarra M (2016a). Anti-Inflammatory Activity of *Citrus bergamia* Derivatives: Where Do We Stand? Molecules 21(10) E1273. doi: 10.3390/molecules21101273.

Ferlazzo N, Cirmi S, Russo M, Trapasso E, Ursino MR, Lombardo GE, Gangemi S, Calapai G, Navarra M (2016b). NF-κB mediates the antiproliferative and proapoptotic effects of bergamot juice in HepG2 cells. Life Sci 146:81-91. doi: 10.1016/j.lfs.2015.12.040.

Fialkow L, Wang Y, Downey GP (2007). Reactive oxygen and nitrogen species as signaling molecules regulating neutrophil function. Free Radic Biol Med 42(2):153-64. doi: 10.1016/j.freeradbiomed.2006.09.030.

Georganopoulou DG, Chang L, Nam JM, Thaxton CS, Mufson EJ, Klein WL, Mirkin CA (2005). Nanoparticle-based detection in cerebral spinal fluid of a soluble pathogenic biomarker for Alzheimer's disease. Proc Natl Acad Sci U S A 102(7):2273-6. doi: 10.1073/pnas.0409336102.

Giri RK, Selvaraj SK, Kalra VK (2003). Amyloid peptide-induced cytokine and chemokine expression in THP-1 monocytes is blocked by small inhibitory RNA duplexes for early growth response-1 messenger RNA. J Immunol 170(10):5281-94. doi: 10.4049/jimmunol.170.10.5281.

Golden TR, Hinerfeld DA, Melov S (2002). Oxidative stress and aging: beyond correlation. Aging Cell 1(2):117-23.

González R, Ballester I, López-Posadas R, Suárez MD, Zarzuelo A, Martínez-Augustin O, Sánchez de Medina F (2011). Effects of flavonoids and other polyphenols on inflammation. Crit Rev Food Sci Nutr 51(4):331-62. doi: 10.1080/10408390903584094.

Hegde PS, White IR, Debouck C (2004). Interplay of transcriptomics and proteomics. Drug Discov Today 9(2 Suppl): S53–6.

Heneka MT, O'Banion MK, Terwel D, Kummer MP (2010). Neuroinflammatory processes in Alzheimer's disease. J Neural Transm (Vienna) 117(8):919-47. doi: 10.1007/s00702-010-0438-z.

Hickey WF, Kimura H (1988). Perivascular microglial cells of the CNS are bone marrow-derived and present antigen *in vivo*. Science 239(4837):290-2. doi: 10.1126/science.3276004.

Hsu JY, Chu JJ, Chou MC, Chen YW (2013). Dioscorin pre-treatment protects A549 human airway epithelial cells from hydrogen peroxide-induced oxidative stress. Inflammation 36(5):1013-9. doi: 10.1007/s10753-013-9633-z.

Kang R, Tang D, Livesey KM, Schapiro NE, Lotze MT, Zeh HJ 3rd (2011). The Receptor for Advanced Glycation End-products (RAGE) protects pancreatic tumor cells against oxidative injury. Antioxid Redox Signal 15(8):2175-84. doi: 10.1089/ars.2010.3378.

Kim D, Kim JY (2014) Anti-CD14 antibody reduces LPS responsiveness via TLR4 internalization in human monocytes. Mol Immunol 57(2): 210–5. doi: doi: 10.1016/j.molimm.2013.09.009.

Kim DI, Lee SJ, Lee SB, Park K, Kim WJ, Moon SK (2008). Requirement for Ras/Raf/ERK pathway in naringin-induced G1-cell-cycle arrest via p21WAF1 expression. Carcinogenesis 29(9):1701-9. doi: 10.1093/carcin/bgn055.

Kim YS, Young MR, Bobe G, Colburn NH, Milner JA (2009). Bioactive food components, inflammatory targets, and cancer prevention. Cancer Prev Res (Phila) 2(3):200-8. doi: 10.1158/1940-6207.

Klegeris A, Walker DG, McGeer PL (1997). Interaction of Alzheimer beta-amyloid peptide with the human monocytic cell line THP-1 results in a protein kinase C-dependent secretion of tumor necrosis factor-alpha. Brain Res 747(1):114-21. doi: 10.1016/S0006-8993(96)01229-2.

Knaapen AM, Shi T, Borm PJ, Schins RP (2002). Soluble metals as well as the insoluble particle fraction are involved in cellular DNA damage induced by particulate matter. Mol Cell Biochem 234-235(1-2):317-26.

Kumar H, Kim IS, More SV, Kim BW, Choi DK (2014). Natural product-derived pharmacological modulators of Nrf2/ARE pathway for chronic diseases. Nat Prod Rep 31(1):109-39. doi: 10.1039/c3np70065h.

Kumar S, Pandey AK (2013). Chemistry and biological activities of flavonoids: an overview. Scientific World Journal 2013:162750. doi: 10.1155/2013/162750.

Kumar S and Pandey AK (2015). Free radicals: health implications and their mitigation by herbals. British Journal of Medicine and Medical Research 7(6): 438-457. doi: 10.9734/BJMMR/2015/16284.

Lee J, Giordano S, Zhang J (2012). Autophagy, mitochondria and oxidative stress: cross-talk and redox signalling. Biochem J 441(2):523-40. doi: 10.1042/BJ20111451.

Lee EJ, Moon GS, Choi WS, Kim WJ, Moon SK (2008). Naringin-induced p21WAF1-mediated G(1)-phase cell cycle arrest via activation of the Ras/Raf/ERK signaling

pathway in vascular smooth muscle cells. Food Chem Toxicol 46(12):3800-7. doi: 10.1016/j.fct.2008.10.002.

Li F, Ye L, Lin SM, Leung LK (2011). Dietary flavones and flavonones display differential effects on aromatase (CYP19) transcription in the breast cancer cells MCF-7. Mol Cell Endocrinol 344(1-2):51-8. doi: 10.1016/j.mce.2011.06.024.

Lioi AB, Rodriguez AL, Funderburg NT, Feng Z, Weinberg A, Sieg SF (2012). Membrane damage and repair in primary monocytes exposed to human β-defensin-3. J Leukoc Biol 92(5):1083-91. doi: 10.1189/jlb.0112046.

Liu RH (2004). Potential synergy of phytochemicals in cancer prevention: mechanism of action. J Nutr 134(12 Suppl):3479S-3485S.

MacNee W (2001). Oxidative stress and lung inflammation in airways disease. Eur J Pharmacol 429(1-3):195-207.

Manthey JA, Grohmann K, Guthrie N (2001). Biological properties of citrus flavonoids pertaining to cancer and inflammation. Curr Med Chem 8(2):135-53.

Mantovani A, Pierotti MA (2008). Cancer and inflammation: a complex relationship. Cancer Lett 267(2):180-1. doi: 10.1016/j.canlet.2008.05.003.

Marino A, Paterniti I, Cordaro M, Morabito R, Campolo M, Navarra M, Esposito E, Cuzzocrea S (2015). Role of natural antioxidants and potential use of bergamot in treating rheumatoid arthritis. PharmaNutrition 3(2):53-59. doi: 10.1016/j.phanu.2015.03.002.

Martorana M, Arcoraci T, Rizza L, Cristani M, Bonina FP, Saija A, Trombetta D, Tomaino A (2013). *In vitro* antioxidant and *in vivo* photoprotective effect of pistachio (*Pistacia vera* L., variety Bronte) seed and skin extracts. Fitoterapia 85:41-8. doi: 10.1016/j.fitote.2012.12.032.

Masella R, Di Benedetto R, Varì R, Filesi C, Giovannini C (2005). Novel mechanisms of natural antioxidant compounds in biological systems: involvement of glutathione and glutathione-related enzymes. J Nutr Biochem 16(10):577-86. doi: 10.1016/j.jnutbio.2005.05.013.

McGeer EG, McGeer PL (2010). Neuroinflammation in Alzheimer's disease and mild cognitive impairment: a field in its infancy. J Alzheimers Dis 19(1):355-61. doi: 10.3233/JAD-2010-1219.

Medzhitov R (2008). Origin and physiological roles of inflammation. Nature 454(7203):428-35. doi: 10.1038/nature07201.

Miceli N, Mondello MR, Monforte MT, Sdrafkakis V, Dugo P, Crupi ML, Taviano MF, De Pasquale R, Trovato A (2007). Hypolipidemic effects of *Citrus bergamia* Risso et Poiteau juice in rats fed a hypercholesterolemic diet. J Agric Food Chem 55(26):10671-7. doi: 10.1021/jf071772i.

Middleton E Jr, Kandaswami C, Theoharides TC (2000). The effects of plant flavonoids on mammalian cells: implications for inflammation, heart disease, and cancer. Pharmacol Rev 52(4):673-751.

Mittal M, Siddiqui MR, Tran K, Reddy SP, Malik AB (2014). Reactive oxygen species in inflammation and tissue injury. Antioxid Redox Signal 20(7):1126-67. doi: 10.1089/ars.2012.5149.

Mladěnka P, Macáková K, Filipský T, Zatloukalová L, Jahodář L, Bovicelli P, Silvestri IP, Hrdina R, Saso L. (2011). *In vitro* analysis of iron chelating activity of flavonoids. J Inorg Biochem 105(5):693-701. doi: 10.1016/j.jinorgbio.2011.02.003.

Mollace V, Sacco I, Janda E, Malara C, Ventrice D, Colica C, Visalli V, Muscoli S, Ragusa S, Muscoli C, Rotiroti D, Romeo F (2011). Hypolipemic and hypoglycaemic activity of bergamot polyphenols: from animal models to human studies. Fitoterapia 82(3): 309–316. doi: 10.1016/j.fitote.2010.10.014.

Nair J, De Flora S, Izzotti A, Bartsch H (2007). Lipid peroxidation-derived etheno-DNA adducts in human atherosclerotic lesions. Mutat Res 621(1-2):95-105. doi: 10.1016/j.mrfmmm.2007.02.013.

Navarra M, Celano M, Maiuolo J, Schenone S, Botta M, Angelucci A, Bramanti P, Russo D (2010). Antiproliferative and pro-apoptotic effects afforded by novel Src-kinase

inhibitors in human neuroblastoma cells. BMC Cancer 10:602. doi: 10.1186/1471-2407-10-602.

Navarra M, Mannucci C, Delbò M, Calapai G (2015). *Citrus bergamia* essential oil: from basic research to clinical application. Front Pharmacol 6:36. doi: 10.3389/fphar.2015.00036.

Navarra M, Ursino MR, Ferlazzo N, Russo M, Schumacher U, Valentiner U (2014). Effect of *Citrus bergamia* juice on human neuroblastoma cells *in vitro* and in metastatic xenograft models. Fitoterapia 95: 83–92. doi: 10.1016/j.fitote.2014.02.009.

Nie YC, Wu H, Li PB, Xie LM, Luo YL, Shen JG, Su WW (2012). Naringin attenuates EGF-induced MUC5AC secretion in A549 cells by suppressing the cooperative activities of MAPKs-AP-1 and IKKs-IκB-NF-κB signaling pathways. Eur J Pharmacol 690(1-3):207-13. doi: 10.1016/j.ejphar.2012.06.040.

Oliveira-Marques V, Marinho HS, Cyrne L, Antunes F (2009). Role of hydrogen peroxide in NF-kappaB activation: from inducer to modulator. Antioxid Redox Signal 11(9):2223-43. doi: 10.1089/ARS.2009.2601.

Paredi P, Kharitonov SA, Leak D, Ward S, Cramer D, Barnes PJ (2000). Exhaled ethane, a marker of lipid peroxidation, is elevated in chronic obstructive pulmonary disease. Am J Respir Crit Care Med 162(2 Pt 1):369-73. doi: 10.1164/ajrccm.162.2.9909025.

Parhiz H, Roohbakhsh A, Soltani F, Rezaee R, Iranshahi M (2015). Antioxidant and anti-inflammatory properties of the *citrus* flavonoids hesperidin and hesperetin: an updated review of their molecular mechanisms and experimental models. Phytother Res 29(3):323-31. doi: 10.1002/ptr.5256.

Picerno I, Chirico C, Condello S, Visalli G, Ferlazzo N, Gorgone G, Caccamo D, Ientile R (2006). Homocysteine induces DNA damage and alterations in proliferative capacity of T-lymphocytes: a model for immunosenescence? Biogerontology 8(2):111-9. doi: 10.1007/s10522-006-9040-z.

Pollard SE, Whiteman M, Spencer JP (2006). Modulation of peroxynitrite-induced fibroblast injury by hesperetin: a role for intracellular scavenging and modulation of

ERK signalling. Biochem Biophys Res Commun 347(4):916-23. doi: 10.1016/j.bbrc.2006.06.153.

Rahman I (2005). Oxidative stress in pathogenesis of chronic obstructive pulmonary disease: cellular and molecular mechanisms. Cell Biochem Biophys 43(1):167-88. doi: 10.1385/CBB:43:1:167.

Rapisarda A and Germanò M P (2013). *Citrus bergamia* Risso and Poiteau botanical classification, morphology and anatomy. *Citrus bergamia*: Bergamot and its Derivatives, eds G. Dugo and I. Bonaccorsi (Boka Raton, FL: CCR Press), 9–11.

Rice-Evans CA, Miller NJ, Paganga G (1997). Antioxidant properties of phenolic compounds. Trends in Plant Science 2(4):152–159. doi:10.1016/S1360-1385(97)01018-2.

Roman J, Ritzenthaler JD, Fenton MJ, Roser S, Schuyler W (2000). Transcriptional regulation of the human interleukin 1beta gene by fibronectin: role of protein kinase C and activator protein 1 (AP-1). Cytokine 12(11):1581-96. doi: 10.1006/cyto.2000.0759.

Ross JA, Kasum CM (2002). Dietary flavonoids: bioavailability, metabolic effects, and safety. Annu Rev Nutr 22:19-34. doi: 10.1146/annurev.nutr.22.111401.144957.

Sommella E, Pepe G, Pagano F, Tenore GC, Dugo P, Manfra M, Campiglia P (2013). Ultrahigh performance liquid chromatography with ion-trap TOF-MS for the fast characterization of flavonoids in Citrus bergamia juice. J Sep Sci 36(20):3351-5. doi: 10.1002/jssc.201300591.

Santangelo C, Varì R, Scazzocchio B, Di Benedetto R, Filesi C, Masella R (2007). Polyphenols, intracellular signalling and inflammation. Ann Ist Super Sanita 43(4):394-405.

Saresella M, Marventano I, Calabrese E, Piancone F, Rainone V, Gatti A, Alberoni M, Nemni R, Clerici M (2014). A complex proinflammatory role for peripheral monocytes in Alzheimer's disease. J Alzheimers Dis 38(2):403-13. doi: 10.3233/JAD-131160.

Sakharwade SC, Sharma PK, Mukhopadhaya A (2013). Vibrio cholerae porin OmpU induces pro-inflammatory responses, but down-regulates LPS-mediated effects in RAW

264.7, THP-1 and human PBMCs. PLoS One 8(9):e76583. doi: 10.1371/journal.pone.0076583.

Sarkar FH, Li Y, Wang Z, Kong D (2009). Cellular signaling perturbation by natural products. Cell Signal 21(11):1541-7. doi: 10.1016/j.cellsig.2009.03.009.

Schildberger A, Rossmanith E, Eichhorn T, Strassl K, Weber V (2013). Monocytes, peripheral blood mononuclear cells, and THP-1 cells exhibit different cytokine expression patterns following stimulation with lipopolysaccharide. Mediators Inflamm 2013: 697972. doi: 10.1155/2013/697972.

Seidman R, Gitelman I, Sagi O, Horwitz SB, Wolfson M (2001). The role of ERK 1/2 and p38 MAP-kinase pathways in taxol-induced apoptosis in human ovarian carcinoma cells. Exp Cell Res 268(1):84-92. doi: 10.1006/excr.2001.5262.

Selkoe DJ (2001). Alzheimer's disease results from the cerebral accumulation and cytotoxicity of amyloid beta-protein. J Alzheimers Dis 3(1):75-80.

Selkoe DJ (2004). Cell biology of protein misfolding: the examples of Alzheimer's and Parkinson's diseases. Nat Cell Biol 6(11):1054-61. doi: 10.1038/ncb1104-1054.

Sharif O, Bolshakov VN, Raines S, Newham P, Perkins ND. (2007). Transcriptional profiling of the LPS induced NF-kappaB response in macrophages. BMC Immunol 8:1. doi: 10.1186/1471-2172-8-1.

Spencer JP (2007). The interactions of flavonoids within neuronal signalling pathways. Genes Nutr 2(3):257-73. doi: 10.1007/s12263-007-0056-z.

Stone JR, Yang S (2006). Hydrogen peroxide: a signaling messenger. Antioxid Redox Signal 8(3-4):243-70. doi: 10.1089/ars.2006.8.243.

Tabas I, Glass CK (2013). Anti-inflammatory therapy in chronic disease: challenges and opportunities. Science 339(6116):166-72. doi: 10.1126/science.1230720.

Toth PP, Patti AM, Nikolic D, Giglio RV, Castellino G, Biancucci T, Geraci F, David S, Montalto G, Rizvi A, Rizzo M (2016). Bergamot Reduces Plasma Lipids, Atherogenic Small Dense LDL, and Subclinical Atherosclerosis in Subjects with Moderate

Hypercholesterolemia: A 6 Months Prospective Study. Front Pharmacol 6:299. doi: 10.3389/fphar.2015.00299.

Tomaino A, Martorana M, Arcoraci T, Monteleone D, Giovinazzo C, Saija A (2010). Antioxidant activity and phenolic profile of pistachio (*Pistacia vera* L., variety Bronte) seeds and skins. Biochimie 92(9):1115-22. doi: 10.1016/j.biochi.2010.03.027.

Trapp J, Jochum A, Meier R, Saunders L, Marshall B, Kunick C, Verdin E, Goekjian P, Sippl W, Jung M (2006). Adenosine mimetics as inhibitors of NAD+-dependent histone deacetylases, from kinase to sirtuin inhibition. J Med Chem 49(25):7307-16. doi: 10.1021/jm060118b.

Uchihara T, Akiyama H, Kondo H, Ikeda K (1997). Activated microglial cells are colocalized with perivascular deposits of amyloid-beta protein in Alzheimer's disease brain. Stroke 28(10):1948-50. doi: 10.1161/01.STR.28.10.1948.

Visalli G, Ferlazzo N, Cirmi S, Campiglia P, Gangemi S, Di Pietro A, Calapai G, Navarra M (2014). Bergamot juice extract inhibits proliferation by inducing apoptosis in human colon cancer cells. Anticancer Agents Med Chem 14(10):1402-13. doi: 10.2174/1871520614666140829120530.

Vollgraf U, Wegner M, Richter-Landsberg C (1999). Activation of AP-1 and nuclear factor-kappaB transcription factors is involved in hydrogen peroxide-induced apoptotic cell death of oligodendrocytes. J Neurochem 73(6):2501-9. doi: 10.1046/j.1471-4159.1999.0732501.x.

Vukic V, Callaghan D, Walker D, Lue LF, Liu QY, Couraud PO, Romero IA, Weksler B, Stanimirovic DB, Zhang W (2009). Expression of inflammatory genes induced by beta-amyloid peptides in human brain endothelial cells and in Alzheimer's brain is mediated by the JNK-AP1 signaling pathway. Neurobiol Dis 34(1):95-106. doi: 10.1016/j.nbd.2008.12.007.

Wang SS, Chen YT, Chou SW (2005). Inhibition of amyloid fibril formation of beta-amyloid peptides via the amphiphilic surfactants. Biochim Biophys Acta 1741(3):307-13. doi: 10.1016/j.bbadis.2005.05.004.

Xie J, Zhang X, Zhang L (2013). Negative regulation of inflammation by SIRT1. Pharmacol Res 67(1):60-7. doi: 10.1016/j.phrs.2012.10.010.

Yamada A, Akimoto H, Kagawa S, Guillemin GJ, Takikawa O (2009). Proinflammatory cytokine interferon-gamma increases induction of indoleamine 2,3-dioxygenase in monocytic cells primed with amyloid beta peptide 1-42: implications for the pathogenesis of Alzheimer's disease. J Neurochem 110(3):791-800. doi: 10.1111/j.1471-4159.2009.06175.

Yao LH, Jiang YM, Shi J, Tomás-Barberán FA, Datta N, Singanusong R, Chen SS (2004). Flavonoids in food and their health benefits. Plant Foods Hum Nutr 59(3):113-22.

Yao H, Rahman I (2012). Perspectives on translational and therapeutic aspects of SIRT1 in inflammaging and senescence. Biochem Pharmacol 84(10):1332-9. doi: 10.1016/j.bcp.2012.06.031.

Yates SL, Burgess LH, Kocsis-Angle J, Antal JM, Dority MD, Embury PB, Piotrkowski AM, Brunden KR (2000). Amyloid beta and amylin fibrils induce increases in proinflammatory cytokine and chemokine production by THP-1 cells and murine microglia. J Neurochem 74(3):1017-25. doi: 10.1046/j.1471-4159.2000.0741017.

Yoshida H, Takamura N, Shuto T, Ogata K, Tokunaga J, Kawai K, Kai H (2010). The citrus flavonoids hesperetin and naringenin block the lipolytic actions of TNF-alpha in mouse adipocytes. Biochem Biophys Res Commun 394(3):728-32. doi: 10.1016/j.bbrc.2010.03.060.

Zhang K, Tian L, Liu L, Feng Y, Dong YB, Li B, Shang DS, Fang WG, Cao YP, Chen YH (2013). CXCL1 contributes to β-amyloid-induced transendothelial migration of monocytes in Alzheimer's disease. PLoS One 8(8):e72744. doi: 10.1371/journal.pone.0072744.

Zimmermann M, Meyer N (2011). Annexin V/7-AAD staining in keratinocytes. Methods Mol Biol 740:57-63. doi: 10.1007/978-1-61779-108-6_8.